UNIVERSITY OF TARTU
INSTITUTE OF ECOLOGY AND EARTH SCIENCES
DEPARTMENT OF GEOLOGY

Peeter Paaver

Geopolymerization of the Estonian oil shale solid heat carrier retorting waste ash: changes in mineral-chemical composition and uniaxial compressive strength development

BSc thesis

Supervisors: Kalle Kirsimäe
Päärn Paiste

TARTU 2014

Table of Contents

Introduction

The term ”geopolymer” was first used in the 1980s by chemist Joseph Davidovits. It refers to reaction of a solid aluminosilicate with a highly concentrated aqueous alkali hydroxide or silicate solution that produces a synthetic alkali aluminosilicate material generically called a ‘geopolymer’, but probably more appropriately referred to as an example of what is more broadly termed an ‘inorganic polymer’ (Duxson, 2006). These materials can provide comparable performance to traditional cementitious binders in a range of applications, but with the added advantage of significantly reduced greenhouse emissions during their production (Duxson, 2006).

Although the term ‘geopolymer’ is generically used to describe the amorphous to crystalline reaction products from synthesis of alkali aluminosilicates from reaction with alkali hydroxide/alkali silicate solution, geopolymeric gels and composites are also commonly referred to as ‘low-temperature aluminosilicate glass’ (Davidovits, 2011). Geopolymers have also been named after their characteristics as ‘alkali-activated cement’, ‘geocement’, ‘alkali-bonded ceramic’, ‘inorganic polymer concrete’, and ‘hydroceramic’. Despite this variety of nomenclature, these terms all describe materials synthesized utilizing the same chemistry, which can be described as a complex system of coupled alkali mediated dissolution and precipitation reactions in an aqueous reaction substrate (Duxson 2006). The polymerization process involves a substantially fast chemical reaction under alkaline condition on Si-Al minerals and/or glasses, that results in a three-dimensional polymeric chain and ring structure consisting of Si-O-Al-O bonds (Davidovits, 2011)

Depending on the raw material selection and processing conditions, geopolymers can exhibit a wide variety of properties and characteristics, including high compressive strength, low shrinkage, fast or slow setting, acid resistance, fire resistance and low thermal conductivity (Duxson, 2006). Despite this wide variety of commonly boasted attributes, these properties are not necessarily inherent to all geopolymeric formulations. Inorganic polymers should not be considered a universal panacea for all material selection problems, but rather a solution that may be tailored by correct mix and processing design to optimize properties and/or reduce cost for a given application (Duxson, 2006).

Production of ordinary Portland cement results from the calcination of limestone (calcium carbonate) and silico-aluminous material as clay minerals. The production of 1 tonne of

cement directly generates 0.55 tonnes of chemical-CO_2 and requires the combustion of carbon-fuel to yield an additional 0.40 tonnes of carbon dioxide. In rapidly developing countries like China and India, cement production has followed an exponential growth trend over the last few decades (Davidovits, 2011) with consequently increasing carbon dioxide emissions. Therefore, there is a global need for more "greener" solutions in this area.
In terms of identical carbon-dioxide emission, the geopolymer chemistry enables the manufacture of 5 to 10 times more cement than Portland technology, with similar investment and lower energy cost. Introducing geopolymeric cements, not only for environmental uses but also in construction and civil engineering, would reduce carbon-dioxide emission caused by the cement industry by 80 to 90 %. This perspective would allow an unlimited development of concrete in the Third World. (Davidovits, 2011)

Oil shales are widely-spread sedimentary rocks containing bituminous organic matter (Craig et al., 2001) that can be pyrolysed to extract shale oil or burnt directly for power generation. Total world resources of shale oil are conservatively estimated at 4.8 trillion barrels, but production of shale oil is, compared to petroleum, more costly due to mining, processing and environmental costs. Thus only few oil shale deposits are actively used, for example in Estonia, China, Israel and Brazil (World Energy Council 2010). Nevertheless, the declining petroleum resources and increasing prices set oil shales into the position of potentially profitable fossil energy reserves.

The Estonian kukersite oil shale is the largest industrially actively used oil shale resource in the world. Estonian oil shale industry has more than 90 years of experience with large scale oil shale usage (Teedumäe and Raukas, 2006). Annual oil shale mining output in past five years has been 14–17 Mt that covers about two thirds of Estonia's fuel balance (Kattai et al., 2000, Statistics Estonia 2010; IEA, 2010). The majority (about 80%) of mined oil shale is utilised in thermal power plants for electricity and heat generation, while most of the remaining oil shale (19%) is used for retorting shale oil and shale-gas (Ots, 2006).
Oil shale is combusted in thermal power plants (TPP) for electricity and heat production using either pulverized fuel (PF) or circulating fluidized bed (CFB) combustion technology (Ots, 2006). Light-coloured ash forms as a residue at TPPs.

Retorting of shale oil and -gas is performed using either "Kiviter" or solid heat carrier (SHC) process (e.g. "Galoter", "Petroter" or "Enefit" process) (Mõtlep et al., 2007). "Kiviter" process

uses gas as heat carrier, whereas SHC process uses hot spent shale formed in the same retorting process as a heat carrier (Golubev, 2003). During retorting the oil shale is heated in the absence of oxygen to the temperature at which its organic part – kerogen – is decomposed or pyrolysed into gas, condensable oil and solid residue, while the inorganic mineral matrix is retained in the form of spent shale (Koel, 1999). The mineral matter content of oil shale can be as high as 80–90%, but usually stays between 40–50%. The main residue from the oil shale industry is TPP ash, and shale-oil processing residues semi-coke and black ash. At the current production rate, each year 5–7 Mt of ash and nearly 1 Mt of semi-coke are formed in Estonia (Statistics Estonia, 2010).

Oil shale processing wastes have been investigated and used for construction (cement, road construction, building materials), agricultural purposes (liming of fields), as fuel additive and water treatment sorbent (e.g. Pets et al., 1985; Hanni, 1996; Paat, 2002; Kaasik et al., 2008; Kõiv et al., 2010 and many others). However, the secondary use of this waste is limited to less than 5% of its annual production, and thus, most of the waste is landfilled. Total ash amount in the depositories is about 300 Mt (Mõtlep et al., 2007; Mõtlep et al., 2010).

Estonian oil shale industry employs different methods for waste disposal. Oil shale ash from power plants is transported by hydraulic transport in slurry at water/solid ratio 20:1 to the plateau-like sedimentation ponds with current height of >40 m at large power plants. In contrast, shale oil processing residue semi-coke is disposed by dry dumping, i.e. it was transported to semi-coke landfills by conveyer belts/wagons in earlier decades and by trucks today, forming landfills with maximum height reaching about 120 m. Amounts of the black ash residue have been so far much smaller compared to TPP ash/semicoke and until now this residue has been deposited together with TPP ash in sedimentation plateaus.

The shale oil producers in Estonia are shifting their focus on new type and more powerful solid heat carrier (SHC) retorts, and consequently the amount of black ash type of waste increases in the future. At the moment the largest producer, Estonian Energy uses two Enefit 140 SHC plant units with one unit producing 140 tonnes of oil shale oil per hour. Together, two plants produce up to 240 000 tonnes of oil per year. One Enefit 280 SHC plant is currently in final testing phase, and Estonian Energy has plans to build 3-4 additional Enefit 280 plants during the next 15 years, taking oil shale oil production up to potential 1.09 million tonnes per year. Together with oil production plants, an oil processing plant, that has ability to

potentially process 20 000 to 30 000 barrels of oil shale oil per day, is planned to be built in the future (*http://www.energiatalgud.ee/img_auth.php/0/01/P%C3%B6yry._%C3%95litehase_maa-ala_detailplaneeringu_KSH_aruanne_.pdf*).

Motivation of this study is to find new ways and methods for oil shale ash secondary use, specifically as a low-cost building materials. The aim of this thesis is to study and evaluate the potential of kukersite oil shale solid heat carrier retorting waste, black ash, for geopolymer type mortar and cement production. The emphasis is given to development of compression strength in alkali activated black ash in comparison with the self-cementation of the same material obtained upon hydration with plain water.

Properties of solid heat carrier ash

Shale-oil retorting produces two types of waste depending on the technology used – blackish semi-coke from "Kiviter" process and dark grey retorting ash (also known as black ash) from solid heat carrier (SHC) process. Semi-coke is a heterogeneous granular material that is rich in organic residues (up to 10%), including phenols, PAHs and oil products that are potential pollutants with harmful environmental effect (Mõtlep et al., 2007). Although additional recycled gas and air are admitted to the chambers to burn off the organics from the residue at the final stage of retorting (Soone and Doilov, 2003), the residence time is too short to burn off all organics. Black ash, on the other hand, is more alike to combustion ash, and contains only a few percents of organics (Golubev, 2003; Talviste et al., 2013). The reason lies in the different retorting technology: during the SHC process retorting residue is heated up in the presence of oxygen and directed back to the retort chamber. This recirculation ensures that the concentration of organics in black ash stays low, and therefore the SHC technology is considered environmentally more advantageous. SHC technology is also economically beneficial, as it uses unriched oil shale of lower calorific value; at the same time the "Kiviter" process is more demanding as it runs on oil shale of higher calorific value (Ots, 2006).

Physical, chemical and mineralogical properties of SCH retorting ash (black ash) have been earlier studied in Talviste et al. (2013), Sedman (2013) and Talviste (2014). Their studies show that black ash contains several reactive phases (e.g. lime, belite) that can react with water and therefore the hydrated black ash sediment has potentially cementation properties. Ash contains notably low amount (<5%) of lime (CaO) suggesting that carbonation reactions do not contribute much to the stabilization of the sediment. However, black ash contains considerable amount of cement clinker minerals belite and ferrite which form C-S-H gel-like mass providing cementation of the material. Hydration of ferrite (C4AF) occurs rather quickly, but its contribution to the strength is rather subdued (6–8 MPa in pure compound), whereas the belite hydration in cement pastes occurs over 60–90 days, but its final strength peaks at about 40 MPa for pure compound (Mindess et al., 2003). Moreover, upon long term hydration black ash develops another binding phase – hydrocalumite. As the result, the black ash mortars show uniaxial compressive strength values >6 MPa after 90 days after curing in ambient air conditions (Talviste et al., 2013).

Cementation of black ash leads to the small, but steady decrease of voids volume, expressed as void ratio decrease (Talviste, 2014). There are three processes that, as an outcome, are resulting in decreased void ratio: (a) tighter packing of grains due to compression, (b) sedimentation of new minerals in the pore space and (c) decrease of specific gravity of the solid phase. This means that decreased void ratio indicates precipitation of cementing minerals into voids similar to sandstone lithification. It is important to note, that precipitated minerals in black ash do not expand voids but form bonds between solid particles and the absence of massive ettringite and gypsum precipitation in black ash is probably the key factor in that (Talviste, 2014). While the void ratio decreases in the mixture, possibly indicating increasing amount of cementing minerals, the initial void ratio indicates distance between the particles prior to bonding. It is possible that the same amount of cement forms different strength of material, depending on the distance between the particles. Based on these assumptions Talviste (2014) suggested that the strength of black ash is possibly controlled via initial void ratio (porosity). Good cementation behaviour of cementing phases in black ash suggests that although the content of binding phases is lower compared to other oil shale wastes, in long term the cementation bonds are more stable due to hydration of belite and low content of unstable ettringite, which becomes decomposed at pH <10 and would cause stability issues of the waste depositories (Talviste et al., 2013).

Material and Methods

Studied black ash originates from the Petroter SHC retort and was provided by Viru Keemia Grupp AS (Kohtla-Järve, Estonia). Fresh dry black ash was stored in airtight containers prior to analysis. Cementation of the black ash was studied in 4 series of monolithic samples made by mixing dry black ash with the following activators: water, sodium-silicate dilution, sodium hydroxide dilution and sodium silicate + NaOH dilution (Table 1). The maximum water content of the mixtures (that is – at saturation conditions) were used. Cylindrical specimens (2.3 cm in diameter and 3.8 cm in high) of black ash/activator mixtures were prepared and stored in PVC tubes. The samples were stored under ambient conditions. For each mixture 3 parallel specimens were made and tested. All sodium silicate based activator solutions were prepared in a way that the Na_2O content in the additive was 10% (w/w) to normalise the amount of soluble silicate in the mixtures.

Table 1. Composition of mixtures used in experiment. SS – Na-silicate

Mixture	Water/ash	Na_2O/ash	SiO_2/Na_2O
ash - H_2O	0.5		
ash- NaOH	0.5	0.09	
ash - NaOH+SS.	0.5	0.1	2.72
ash - SS.	0.5	0.1	1.5

Self-cementing properties of black ash were evaluated by uniaxial compressive strength tests under continuous loading (20 $kPa \cdot s^{-1}$) until the specimen broke. Compressive strength was measured in three replicas after 7, 28 and 90 days. For testing, cylindrical specimens were removed from the PVC tubes. Altogether 36 compressive strength tests were conducted in the Laboratory of Sedimentology at the Department of Geology, University of Tartu.

Mineral and chemical composition of fresh black ash and solidified samples were examined using X-ray diffractometry on Bruker D8 Advance diffractometer using Cu$K\alpha$ radiation and X-ray fluorescence analysis on Rigaku Primus II spectrometer, respectively. The mineral composition of hardening material was analysed in the specimens used in compressive strength tests, i.e. after 7, 28 and 90 days. Chemical composition was determined from initial fresh ash and samples after 90 days of curing. For XRD and XRF analysis the materials were dried at 105 °C for 2 hours and ground in planetary ball-mill. The quantitative mineral composition of the unoriented powdered samples was modelled using Rietveld method in

Topas 4.0 code. To determine the quantity of the amorphous glassy phase, that is not detected by conventional XRD method, the test specimens were spiked with 10% by mass f ZnO prior XRD measurement. Amorphous phase adsorbs X-rays and causes apparently lower ZnO content in sample than it was added. Its content is calculated from difference of added and measured spike phase assuming the alumosilicate composition of the glass.

Total organic carbon in original fresh black ash was measured as the loss on ignition at 550 °C for 2 hours, and total loss on ignition of all samples was measured at 950 °C for 2 hours.
Scanning electron microscopy imaging of test samples was undertaken on Zeiss EVO MA15 SEM equipped with Oxford AZTEC energy dispersive X-ray analytical system. Samples were analysed both uncoated in variable pressure mode and coated with gold or platinum in high vacuum mode.

Results

Mineral composition

Fresh black ash

Average mineral composition of crystalline and amorphous phases of fresh black ash (Figure 2, Supplement 1) was dominated by calcite (26.8%), quartz (11.7%) and K-feldspar (14.3%). The content of dolomite was on average 8.5%. All these components are also characteristic to raw oil shale. In addition black ash contained secondary phases formed during thermal treatment of oil shale: authigenic Ca-silicates (14%), periclase (7.5%), free lime (2.1%) and oldhamite (3.6%).

Oldhamite is a CaS phase that is particularly characteristic for black ash and does not occur in TPP ashes. Oldhamite forms under oxygen deficiency conditions in reaction between CaO and SO_2. Another mineral indicating oxygen deficiency during black ash formation is partly oxidised Fe-oxide mineral magnetite Fe_3O_4, ($FeO*Fe_2O_3$) while in TPP ashes hematite Fe_2O_3 is typically present. In addition, dehydrated mica-like clay phase was identified in black ash. Content of amorphous glass phase varies in fresh black ash from 3.0 to 7.2 and average content of amorphous phase was 5.7%

Chemical composition of the fresh ash (Table 2, Figure 9) corresponds to the mineral composition of studied samples and is dominated by CaO and SiO_2 that compose on average 32% and 21%, respectively. Content of MgO, Al_2O_3 and Fe_2O_3 in fresh ash is on average 8.2, 5.3 and 3.7%, respectively and the sulphur content is on average 2.0%. Carbon content (C_{total}) is about 7.0% and the content of organic carbon (C_{org}) is 1.5–2.2%.

Black ash – water

Mineral and chemical composition of the black ash and water mixtures is different from the fresh black ash composition because of hydration and possible geopolymerisation reactions (Figure 1 and 2, Supplement 1). Mineral composition of water treated black ash samples after 7 days of hydration is principally similar to the original black ash – carbonate mineral phases (calcite and dolomite) content is about 35%. Content of terrigenous mineral phases (quartz, orthoclase and mica-muscovite) is about 26% and content of secondary calcium silicate phases is about 12.5%, whereas the content of periclase (MgO) is about 2.2% (Figure 1, 2).
The major difference in mineral composition of the hydrated samples after 7 days is the disappearance of oldhamite (CaS) and formation of secondary Ca-Al hydrate phase

hydrocalumite and Ca-Al sulphate-hydrate phase ettringite. In fresh ash the oldhamite content is about 3.6%, but after 7 days of hydration practically all of it has been dissolved. Also the CaO (lime) has practically disappeared after 7 days of hydration and as a result calcium portlandite $Ca(OH)_2$ appears in the mineral composition. The content of hydrocalumite and ettringite after 7 days is, respectively 13.9% and 4.7%. There is also a change in the amorphous phase. Content of the amorphous phase in the fresh ash is about 5% and in the 7th day sample about 2%. However the determination of the amorphous phase content is not very precise and the relative error can be as high as 30 to 50% and this change can be just a variation. After 28 and 90 days the changes in the mineral composition of the water hydrated samples compared to composition of the mixture after 7 days are rather small. Only portlandite nearly disappears and content of calcite somewhat increases, evidently due to portlandite carbonation. Also there is a slight increase in ettringite up to 7.6% and the amorphous phase is practically absent, less than 1% after 28 and 90 days.

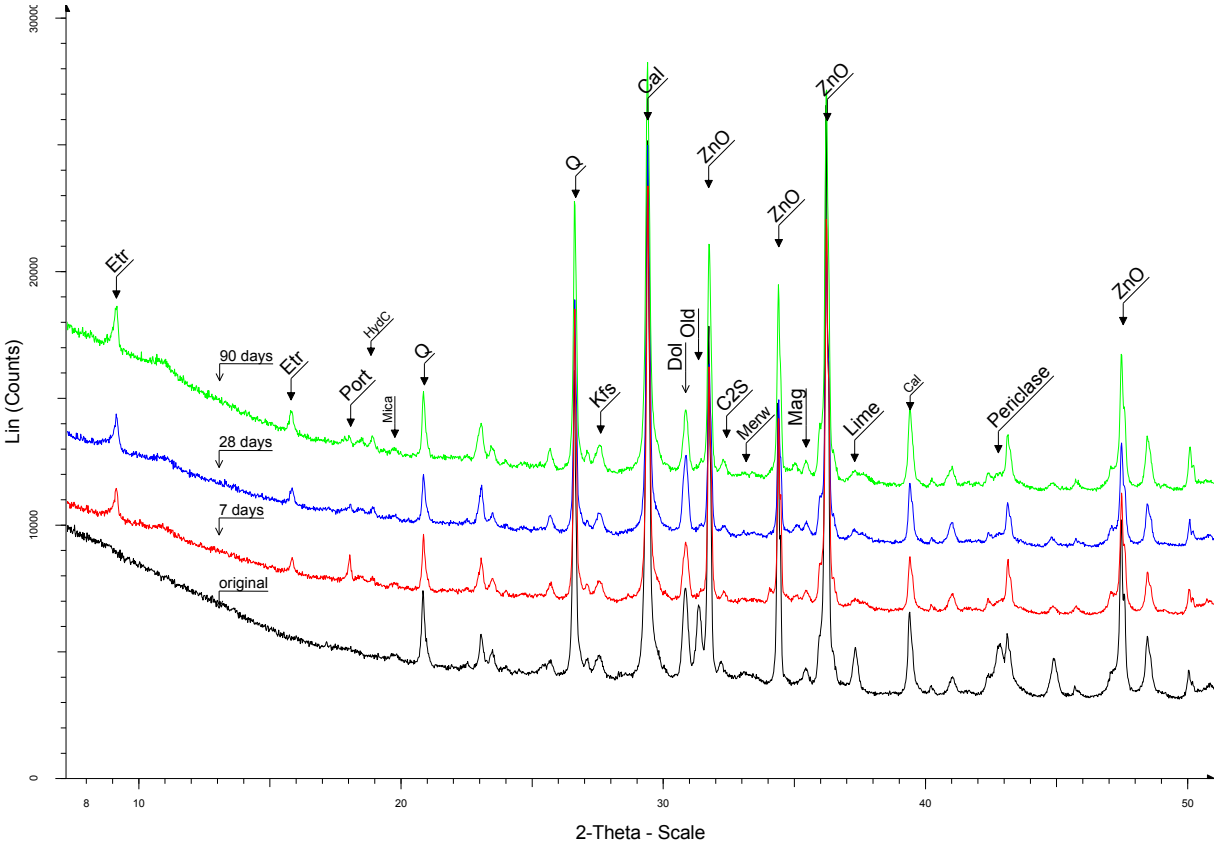

Figure 1. XRD pattern of original black ash and water mixtures after 7, 28 and 90 days. Etr – Ettringite, Port – Portlandite. HydC- Hydrocalumite, Mica – Muscovite. Q – Quartz, Kfs – K-felspar, Cal – Calcite, Dol – Dolomite, Old – Oldhamite, C2S – Belite, Merw – Merwinite, Mag – Magnetite, ZnO - Zincite. Horizontal 2-Theta scale is for CuKα radiation.

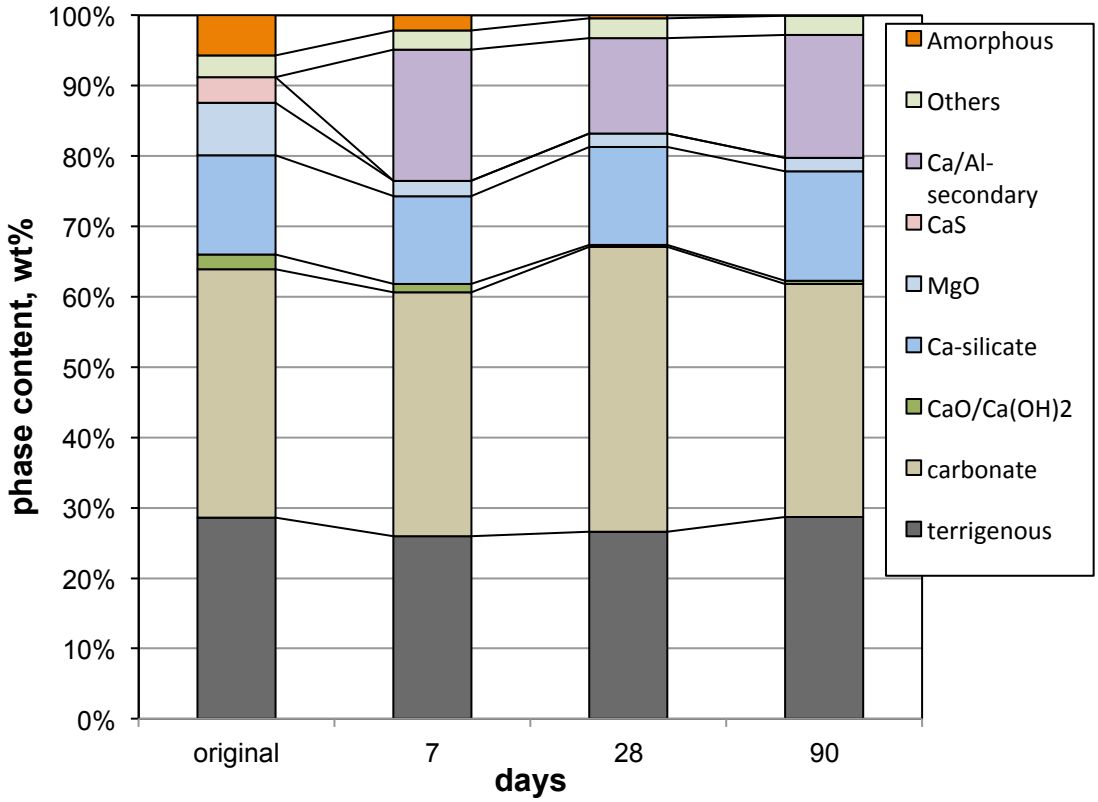

Figure 2.Mineralogical composition of fresh black ash and water mixed samples over 7, 28 and 90 days. Terrigenous minerals – quartz, K-felspar, mica/muscovite; carbonate minerals – calcite, vaterite, dolomite; CaO/Ca(OH)2 – lime, portlandite; Ca-silicate – C2S, merwinite, wollastonite; Ca/Al-secondary – ettringite, hydrocalumite; others – magnetite, hematite, hypsum, anhydrite.

Black ash – NaOH

Mineral composition changes of the samples treated with NaOH dilution are very similar to the ones mixed with water (Figure 3, 4). The content of dominant phases in NaOH treated samples compared with water treated samples differs typically up to 5%. However, there are a few mentionable differences between water and NaOH activated samples. The most important difference compared to the samples treated with water is the absence of ettringite in NaOH activated mixture. Also the content of hydrocalumite is about 4% higher in the 7 day samples and 5 to 7% higher in the 28 and 90 day samples than in specimens mixed with water. Moreover, authigenic clay mineral identified as montmorillonite type smectite appears after 7 days of hydration in low content (0.5%) and in a slightly higher content (2.1%) after 90 days.

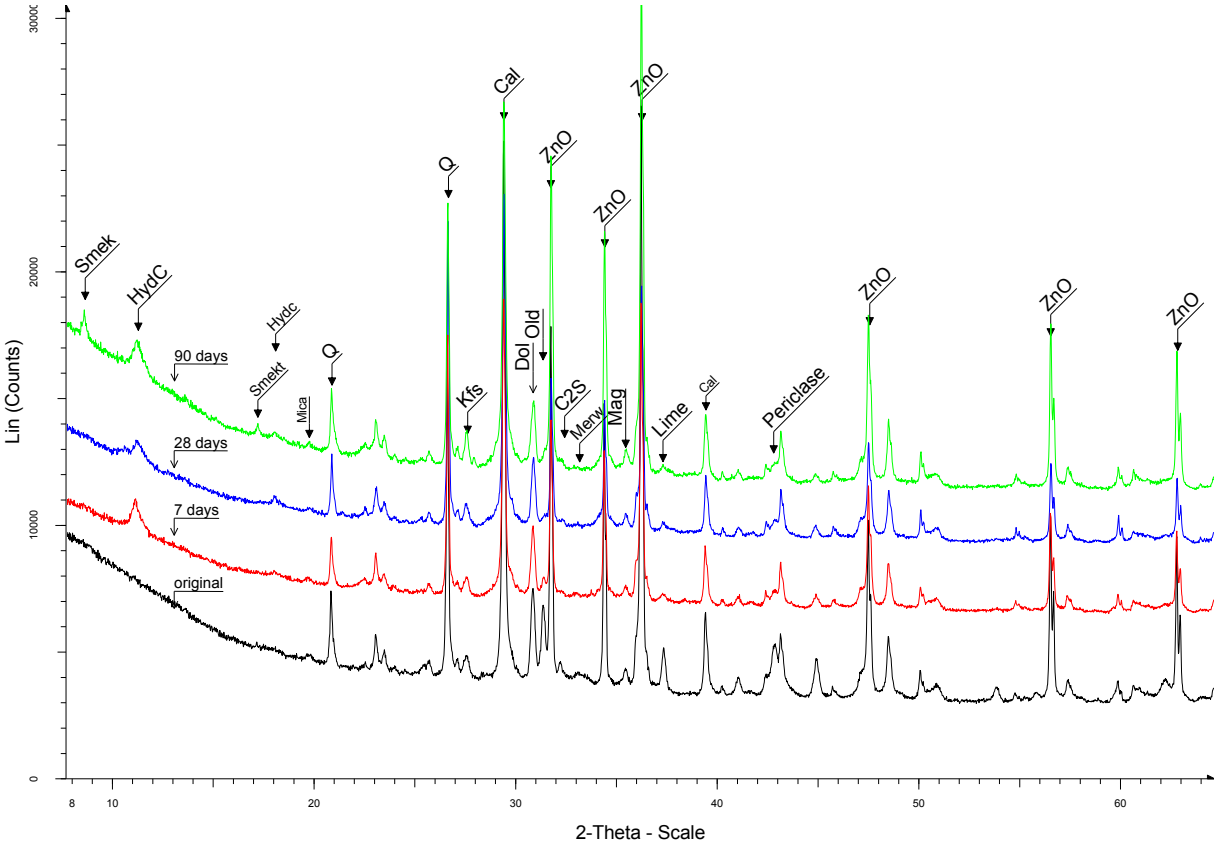

Figure 3. XRD diffractogram of original black ash and NaOH mixtures after 7, 28 and 90 days. For legend see figure 1. Horizontal 2-Theta scale is for CuKα radiation.

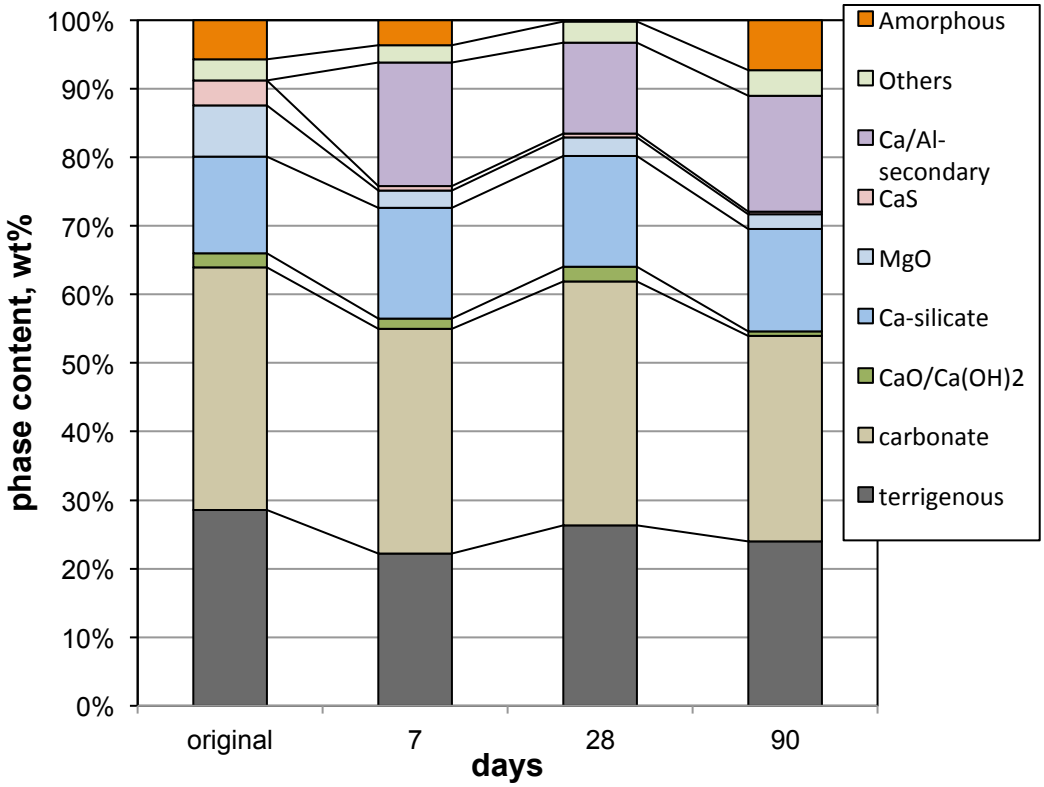

Figure 4. Mineralogical composition of fresh black ash and NaOH activated samples over 7, 28 and 90 days. For legend see figure 2.

There is also a increase of the amorphous phase after 90 days, which could indicate the formation of amorphous geopolymer phase, but as mentioned earlier, the determination of amporphous phase isn't very accurate and there can be a large relative error,. However, the formation of authigenic smectite clay in this mixture indicates dissolution and recrystallizations of Si-and Al-phases. (Figure 3 and 4).

Black ash – Na-silicate and Na-silicate/NaOH

Mineral composition of the black ash specimens mixed with Na-silicate dilution (diluted solution) differs considerably from the samples treated with water or NaOH.

A definitive major change compared to fresh black ash samples and water mixed samples is the massively increased content of the amorphous phase, which has increased from the 5.7% content in the fresh ash to about 30% in 7 days and to 35 and 31 percent in 28 and 90 days, respectively (Figure 5 and 6). This is due to the formation of amorphous Ca-Na-Al-silicate gel from the reaction between Na-silicate solution and minerals present in black ash.

As the result of amorphous phase addition there is a drop in carbonate phases (calcite, vaterite and dolomite) from 35% of the fresh ash composition to about 26% in 7 days and a drop in periclase and oldhamite phases from 7.5% and 3.6% to about 2% and less than 1% respectively over the curing period. CaO(lime) has totally disappeared after the hydration as was also observed in mixtures with water.

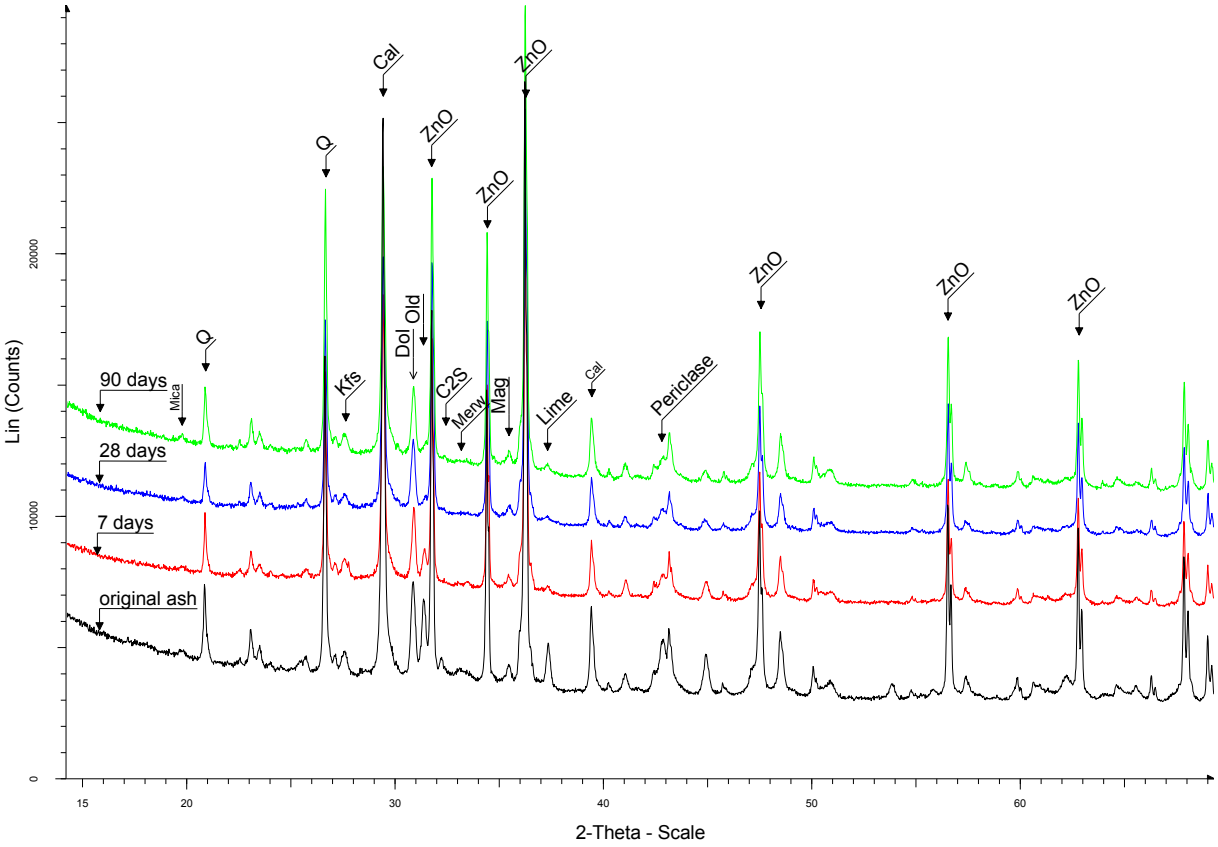

Figure 5 . XRD pattern of original black ash and Na-silicate mixtures after 7, 28 and 90 days. For legend see figure 1. Horizontal 2-Theta scale is for CuKα radiation.

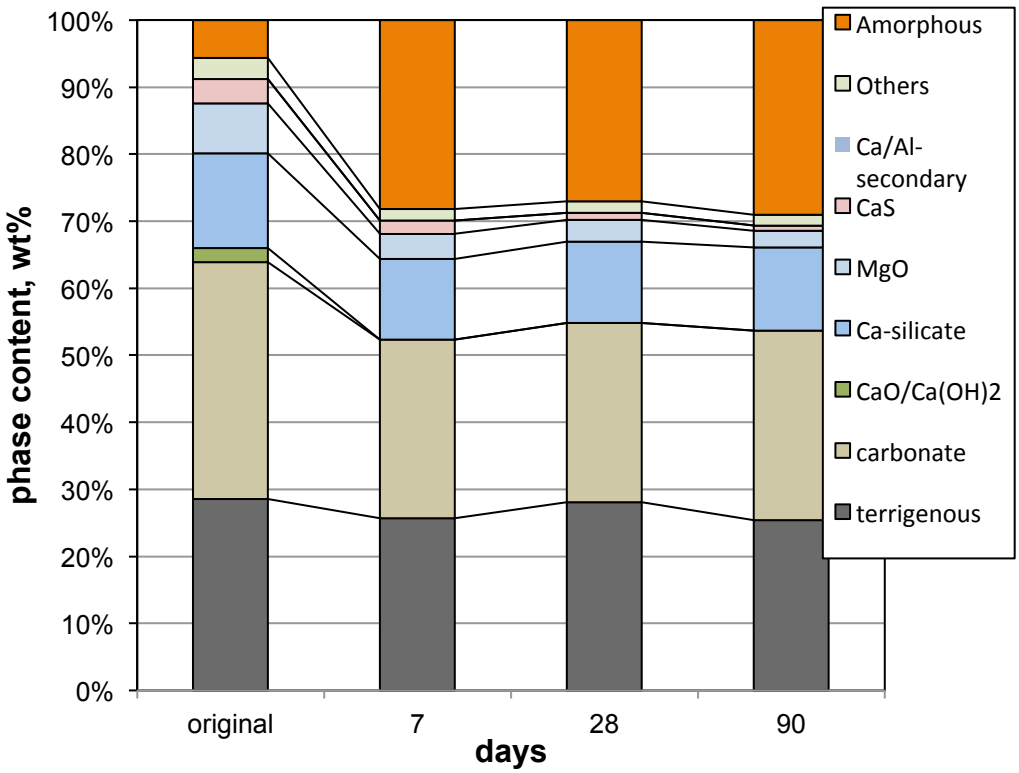

Figure 6. Mineralogical composition of black ash and Na-silicate activated samples. For legend see figure 2.

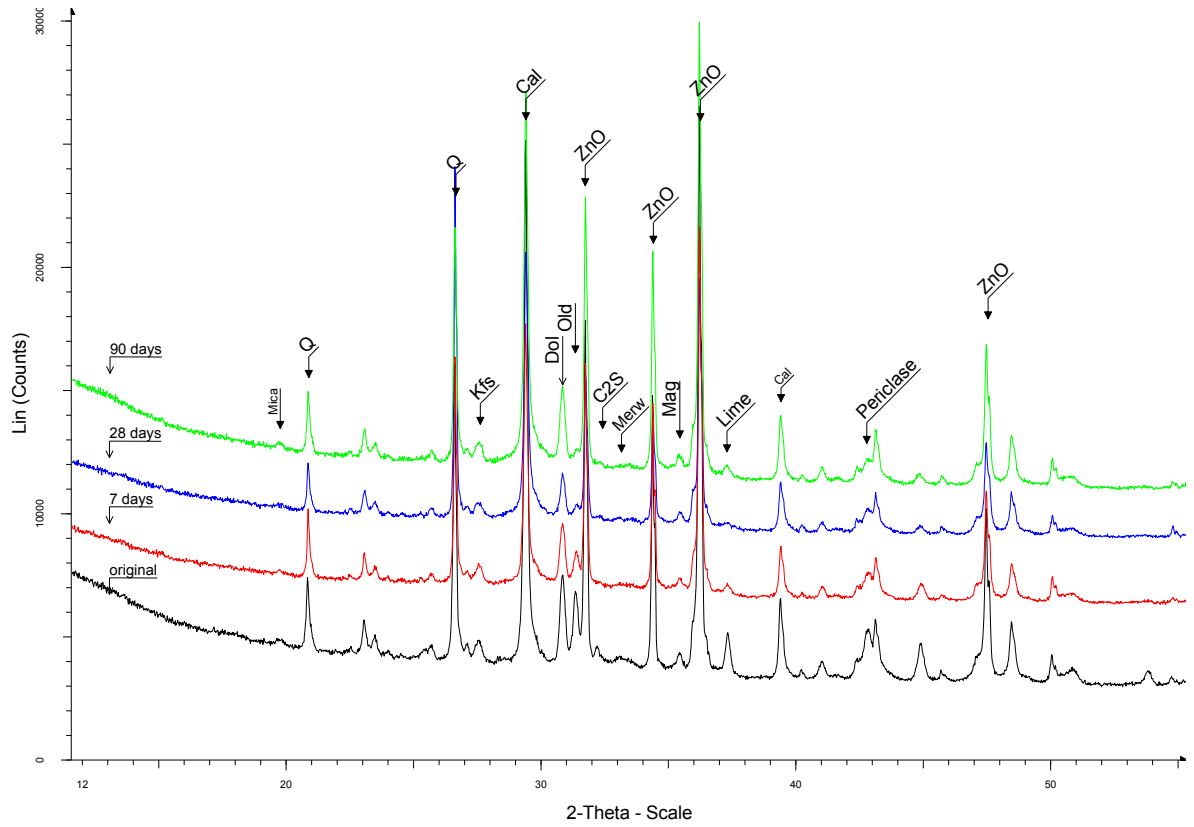

Figure 7. XRD pattern of original black ash and Na-silicate/NaOH mixtures after 7, 28 and 90 days. For legend see figure 1. Horizontal 2-Theta scale is for CuKα radiation.

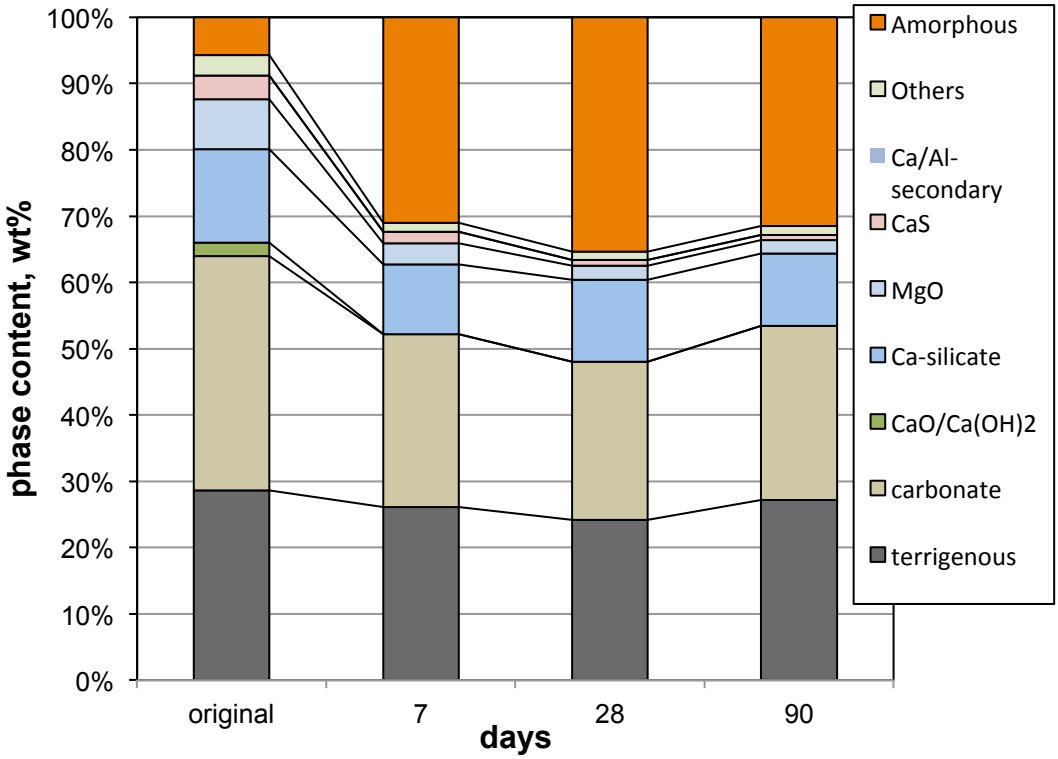

Figure 8. Mineralogical composition of black ash and Na-silicate/NaOH activated samples after 7, 28 and 90 days of curing. For legend see figure 2.

There are no significant mineralogical differences between samples activated by Na-silicate and samples treated with Na-silicate + NaOH dilution. Differences in mineralogical composition in these two different mixtures vary in the range of a few percent (Figure 7, 8) indicating similar changes.

Chemical composition

Chemical composition of studied materials was measured in original fresh ash and after 90 days of curing. The chemical composition of the studied samples corresponds to their treatment method.

In mixture with water the dominant elements are magnesium, calcium and silicon referred as respective oxides (Table 2, Figure 9). During the curing period there have been only slight changes in the chemical composition in the water mixtures. There is an increase in loss on ignition (950 °C) in black ash – water mixture samples (Figure 9) that is obviously due to carbonation of portlandite and capture of atmospheric CO_2 by additional calcite precipitation. This added CO_2 is released during calcite decomposition at temperatures >800 °C.

The changes in NaOH and Na-silicate mixtures are related to addition of Na in the first case and Na and Si in the second case. In the samples mixed with Na-silicate, SiO_2 levels have increased to 32.5% in the sample prepared with Na-silicate and NaOH and to 38% in the sample prepared with only Na-silicate. Other changes include a few percent drop in magnesium and sulphur level and a rise in sodium level in samples mixed with NaOH or Na-silicate.

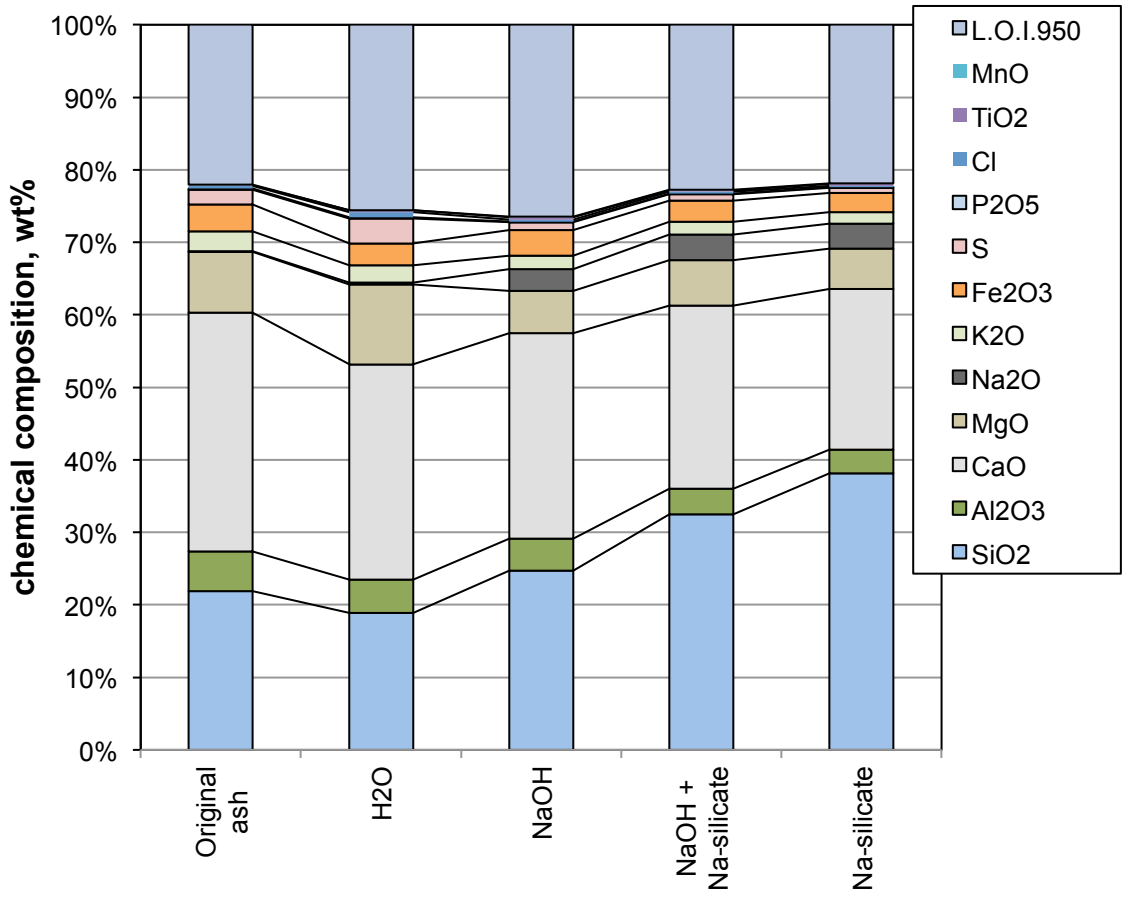

Figure 9. Chemical composition of original ash and all mixtures after 90 days of curing.

Table 2. Chemical composition of black ash and mixtures after 90 days of curing, wt%.

Oxide	Original ash	ash - H2O	ash - NaOH	ash - NaOH + Na-silicate	ash - Na-silicate
SiO2	21.23	18.88	24.67	32.47	38.12
Al2O3	5.27	4.56	4.47	3.57	3.24
TiO2	0.16	0.25	0.32	0.24	0.24
Fe2O3	3.65	3.02	3.47	2.97	2.62
MnO	0.07	0.06	0.06	0.05	0.05
CaO	31.89	29.72	28.26	25.24	22.15
MgO	8.15	11.01	5.84	6.23	5.61
Na2O	0.11	0.24	2.97	3.53	3.43
K2O	2.58	2.38	1.92	1.73	1.56
Cl	0.34	0.67	0.27	0.23	0.21
P2O5	0.11	0.19	0.08	0.07	0.06
S	1.97	3.42	1.11	0.88	0.77
L.O.I. 950 °C	21.33	25.54	26.47	22.74	21.89
Corg	1.86				

Uniaxial compressive strength

Uniaxial compressive strength was measured in 3 replicas of 4 different mixtures after 7, 28 and 90 days.

After 7 days of curing the black ash mixed with Na-silicate dilution achieved very good results with compressive strength reaching over 8 MPa on average and peaking at over 10 MPa (Figure 10). However, after 28 days of curing the compressive strength results dropped under 5 MPa. Although, after 90 days of curing strength results had increased a little, the results still remained low compared to the strengths that this mixture initially achieved. It is important to note that Na-silicate samples were significantly reduced in size already after 7 days of curing and the volume of the Na-silicate treated samples decreased up to 10%.

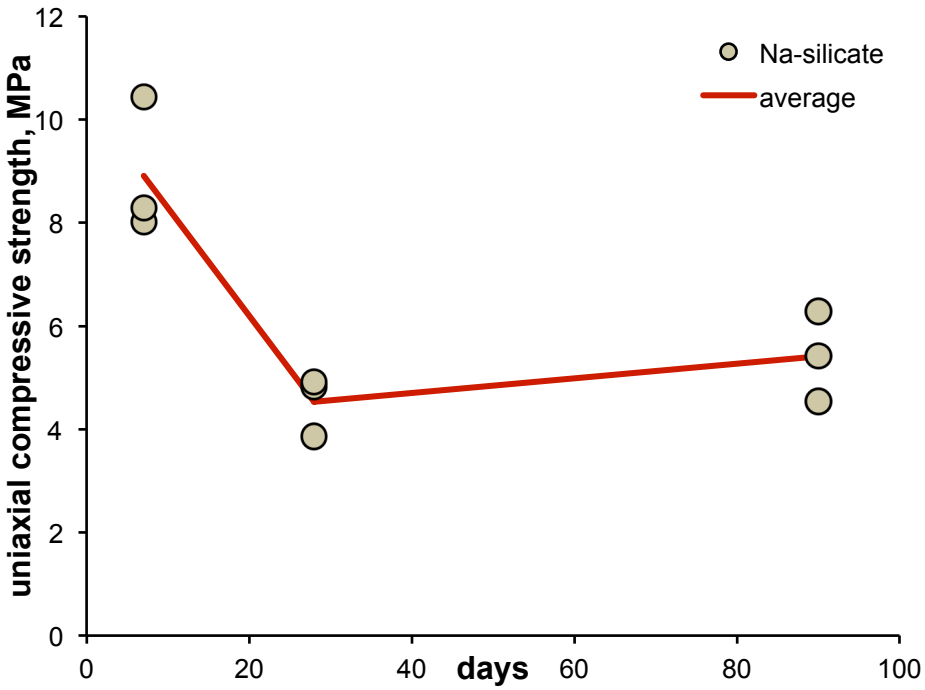

Figure 10. Uniaxial compressive strength values measured in 3 replicas after 7, 28 and 90 days of Na-silicate treated samples.

Mixture of black ash and Na-silicate diluted with NaOH also achieved rather high values after 7 days, from 3.6 to 7.6 MPa. But after 28 days, the increase in strength was quite small – 6 MPa on average. After 90 days the volume of the specimens had decreased similarly to Na-silicate samples and compressive strength results had furthermore dropped under 5 MPa (Figure 11)

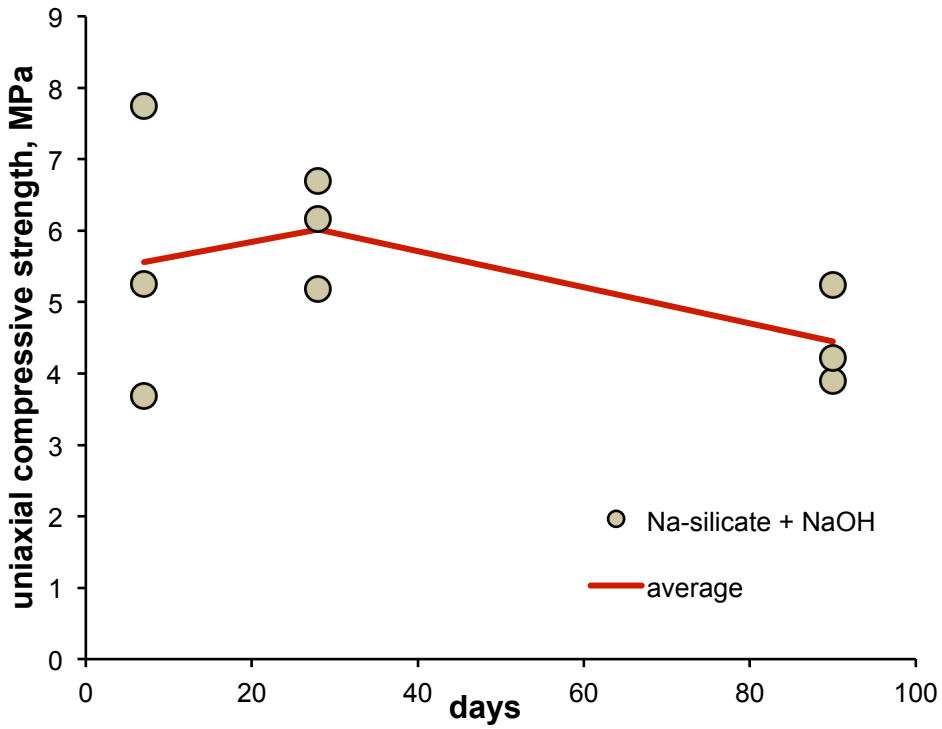

Figure 11. Uniaxial compressive strength values measured in 3 replicas after 7, 28 and 90 days of Na-silicate/NaOH treated samples.

Unlike samples treated with Na-silicate, samples mixed with only NaOH maintained a steady growth in strength over 90 day curing period, but then again these samples still had a very low compressive strength even after 90 days of curing (Figure 12).

After 7 days of curing the uniaxial compressive strength of the black ash NaOH mixtures was on average 1,25 MPa, after 28 days it was only slightly increased to about 1,35 MPa and after 90 days the change was higher to about 4 MPa on average. This would indicate that some geopolymer-like bonds were developed only by 90 days of curing, which agrees with increase in amorphous phase content in these samples after 90 days (Figure 4).

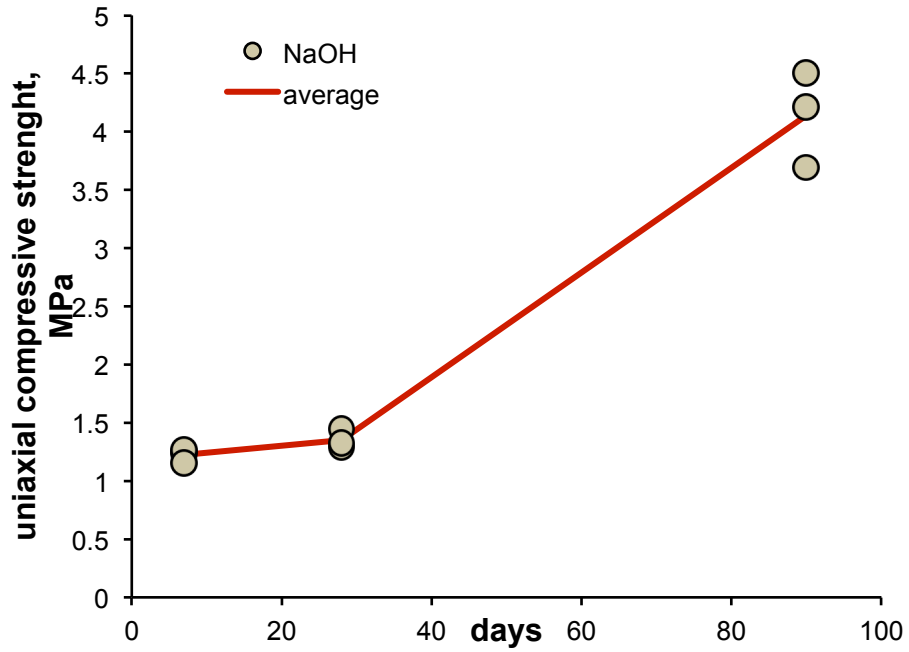

Figure 12. Uniaxial compressive strength values measured in 3 replicas after 7, 28 and 90 days of NaOH treated samples.

Samples that were mixed from black ash and water on the other hand maintained a steady growth over the curing period, but unlike samples treated with NaOH, achieved quite high strength values. After 7 days, samples mixed with water exhibited compressive strengths of only 2 MPa, but after 28 days the samples already show an average strength of almost 6 MPa and after 90 days about 8 MPa with strongest sample peaking at nearly 10 MPa (Figure 13).

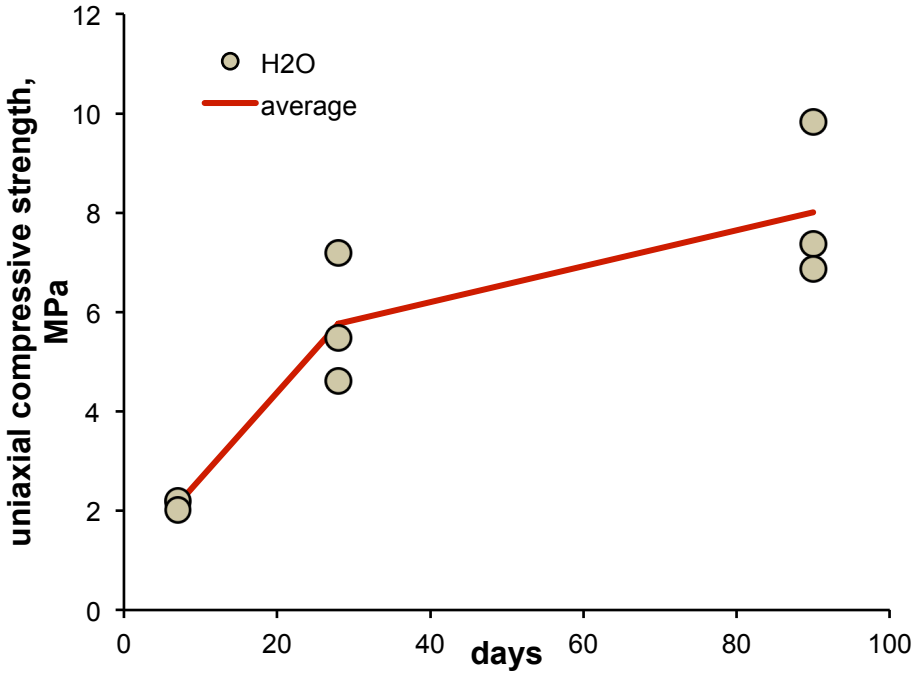

Figure 13. Uniaxial compressive strength values measured in 3 replicas after 7, 28 and 90 days of water treated samples.

Microstructure

SEM imagery of original black ash shows that the material is fine grained with particle size generally less than 60 µm and dominate by fine particles with diameter <20 µm (Figure 14a). The particles are irregular in shape and the finest particles are somewhat aggregated into lumps in 20-30 µm in size (Figure 14b).

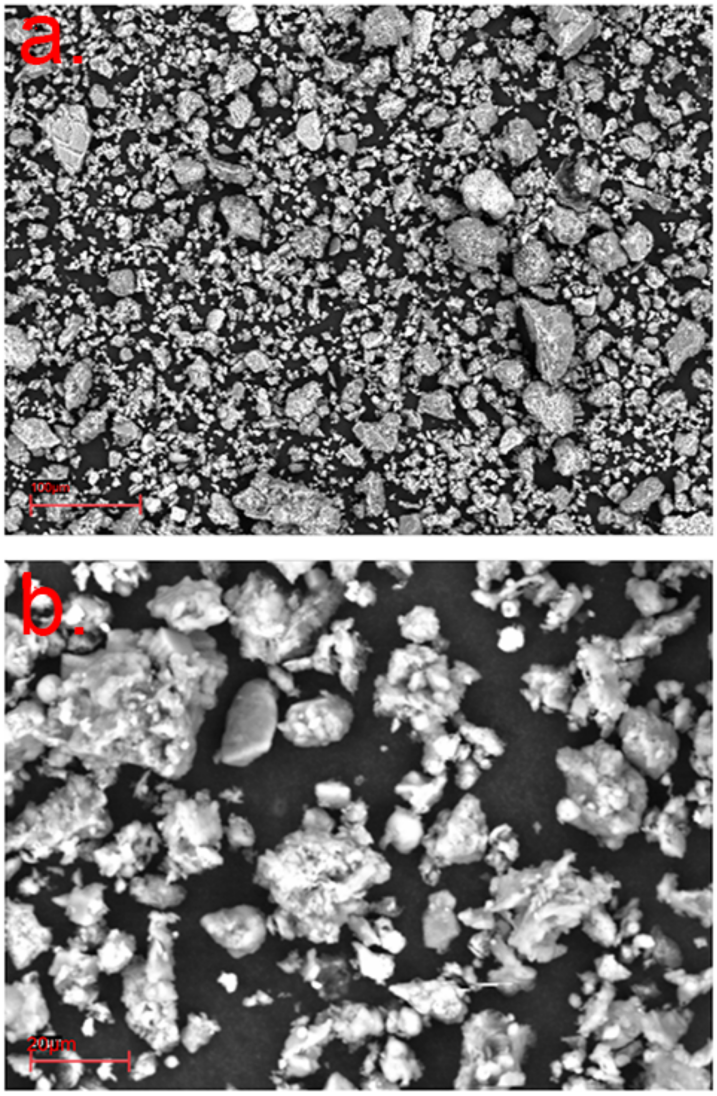

Figure 14. SEM electron images (backscatter – BSE) of fresh black ash.

Microstructure of samples mixed with water (Figure 15 and 16) show intensive cementation and development of secondary Ca-Al and Ca-Al-sulphate minerals in the material pore space. The ash particles are covered by secondary precipitates and bonds between particles are generated by interlocking needle and lath-shape authighenic minerals that can be identified as hydrocalumite and ettringite. Secondary calcite precipitation can also be observed (Figure 16a). There is a significant increase in the density of secondary mineral precipitates when comparing samples after 7 and 90 days of curing (Figure 15 and 16).

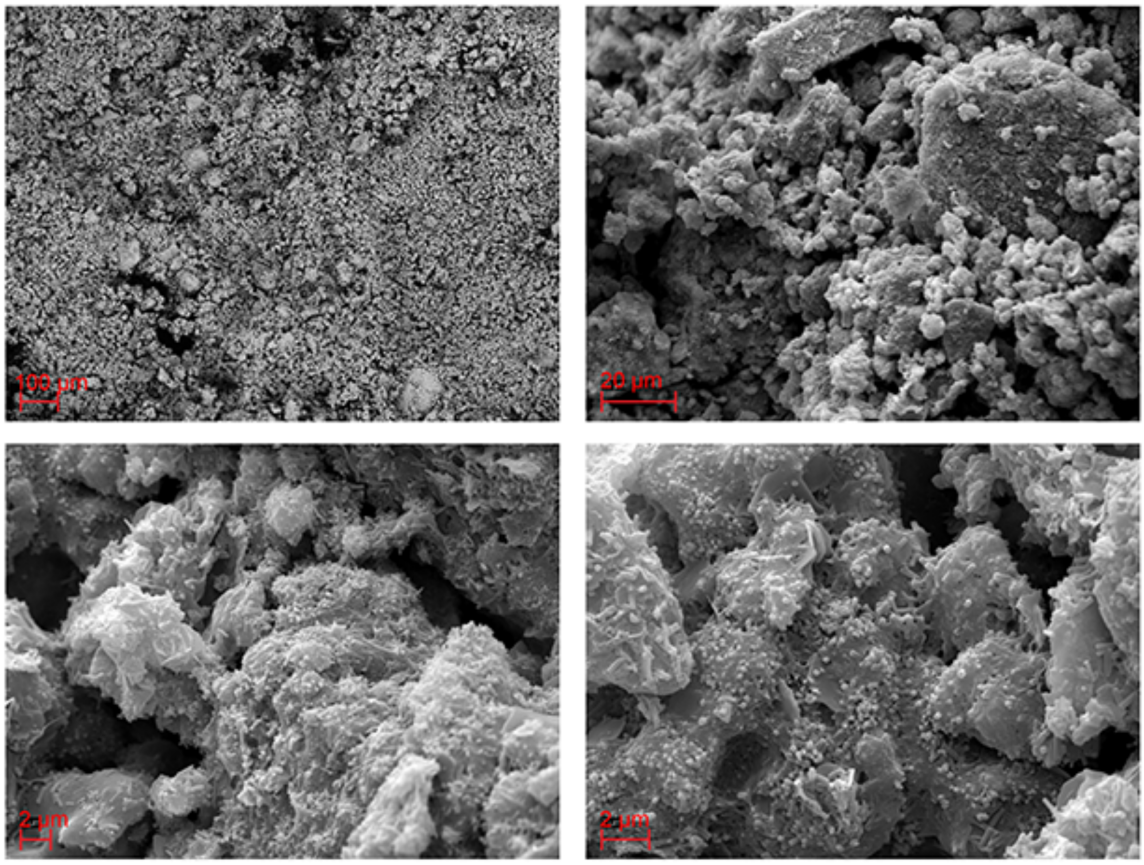

Figure 15. SEM electron images of black ash and water mixture after 7 days of hydration

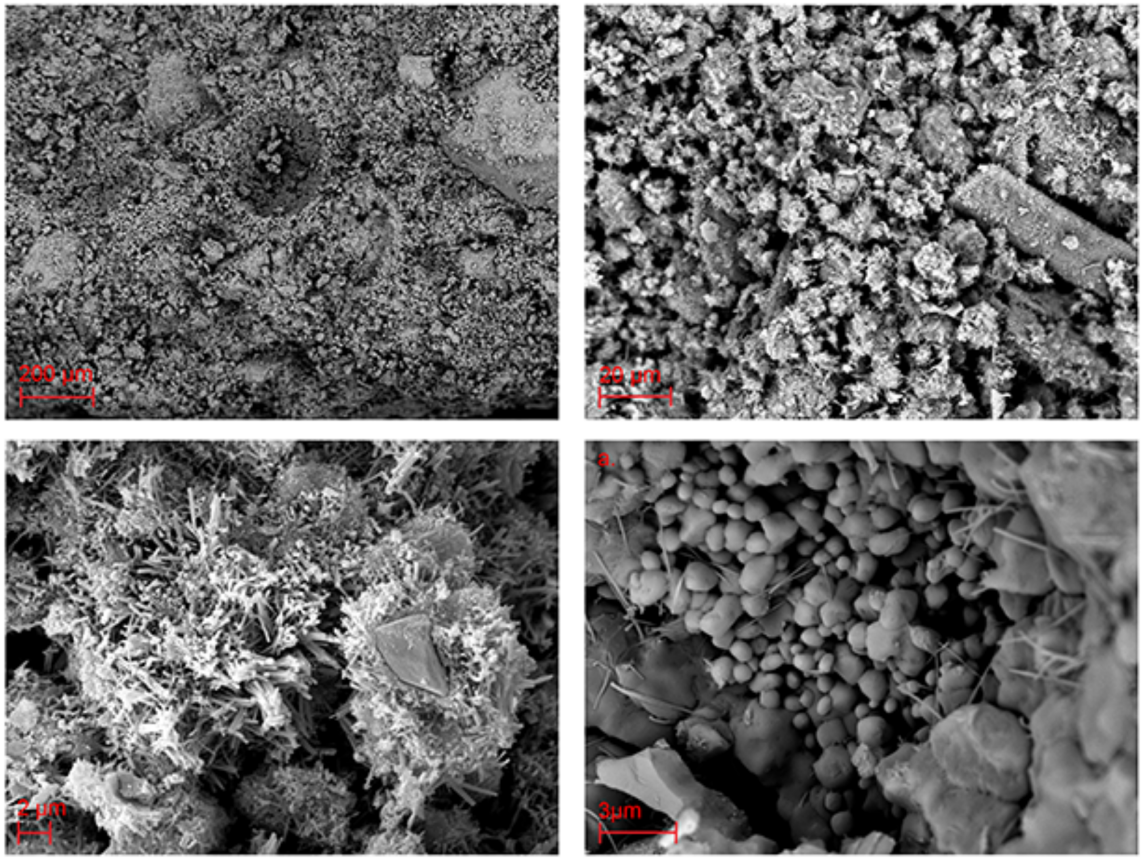

Figure 16. SEM electron images of black ash and water mixture after 90 days of hydration

Mixtures activated with only NaOH show similar microstructure with water mixed samples, but ettringite is missing and pore-space is filled with hydrocalumite platy crystals and crystal aggregates (Figure 17). This finding agrees well with the mineralogical data. Size of the hydrocalumite crystallites is generally 2-5 µm, but in places, larger crystals reaching >10 µ were observed (Figure 17).

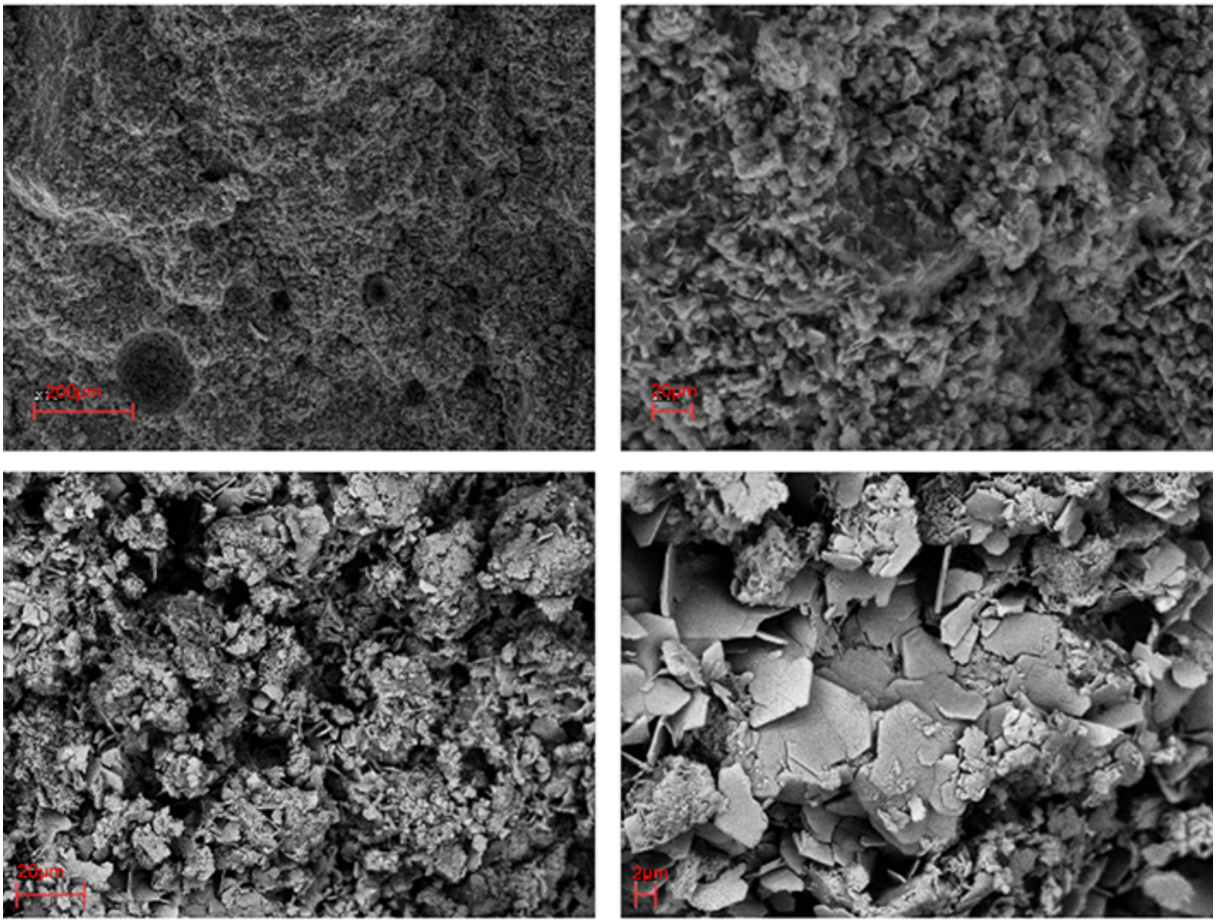

Figure 17. SEM electron images of black ash and NaOH mixture after 90 days.

Microstructure of Na-silicate/NaOH and Na-silicate activated mixtures is considerably different from water and NaOH mixtures and similar to each other (Figure 18 and 19). SEM images show that materials are composed of Ca-Na-Al-silicate gel-like matrix, filling the area between unreacted ash particles. Ca-Na-Al-silicate gel (geopolymerized "glass") is strongly fractured and practically all surfaces are cut with dense fracture networks (Figure 18). Fracturing occurs already in samples after 7 days of curing, but is specifically intense in samples analyzed after 28 and 90 days. However, it must be considered that the development of cracks is also due to dewatering of the gel under vacuum conditions in electron microscope, but the same was observed in low vacuum conditions indicating that the fracturing is not solely induced by the vacuum (Figure 20).

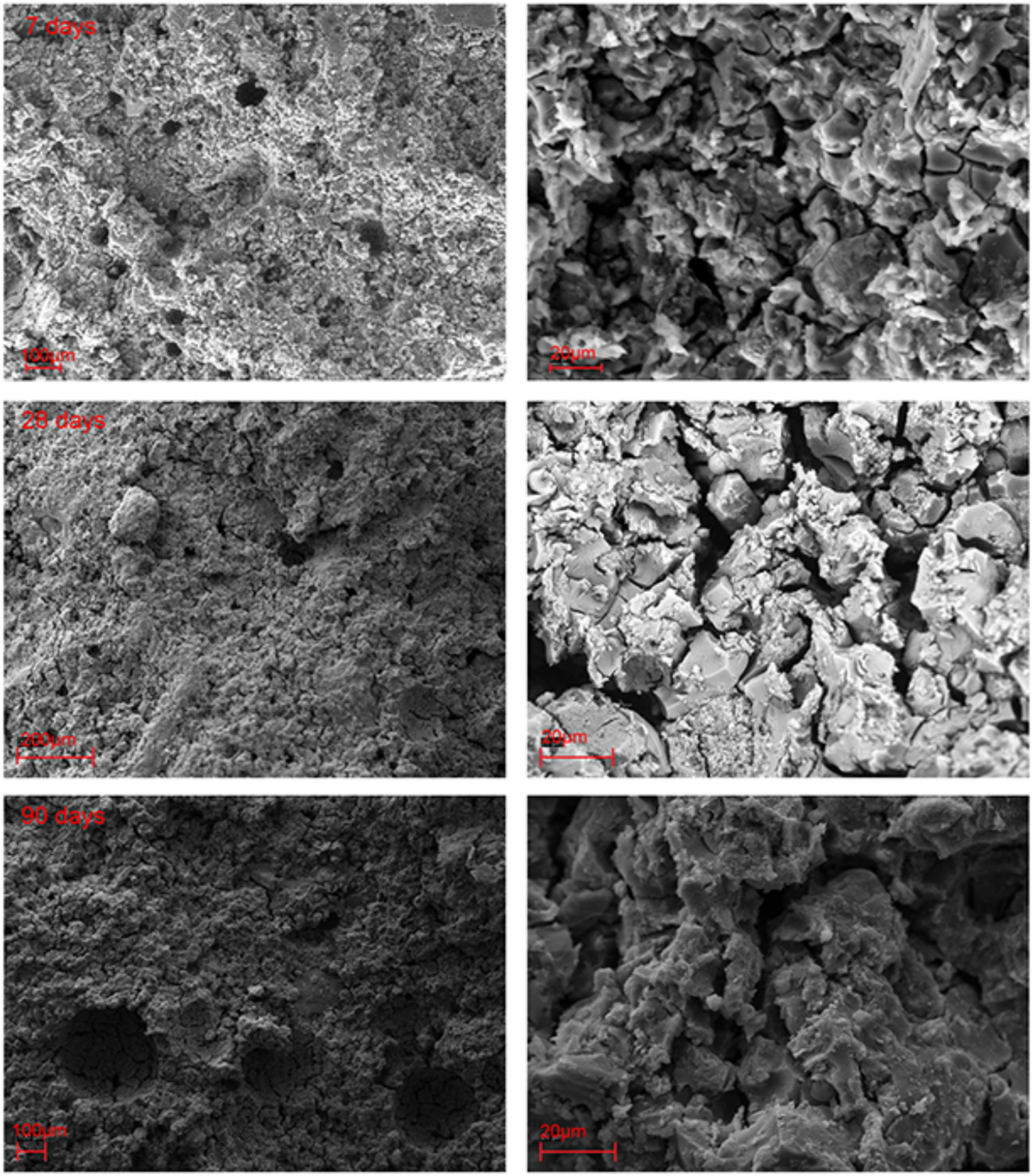

Figure 18. SEM electron images of black ash and Na-silicate mixtures after 7, 28 and 90 days.

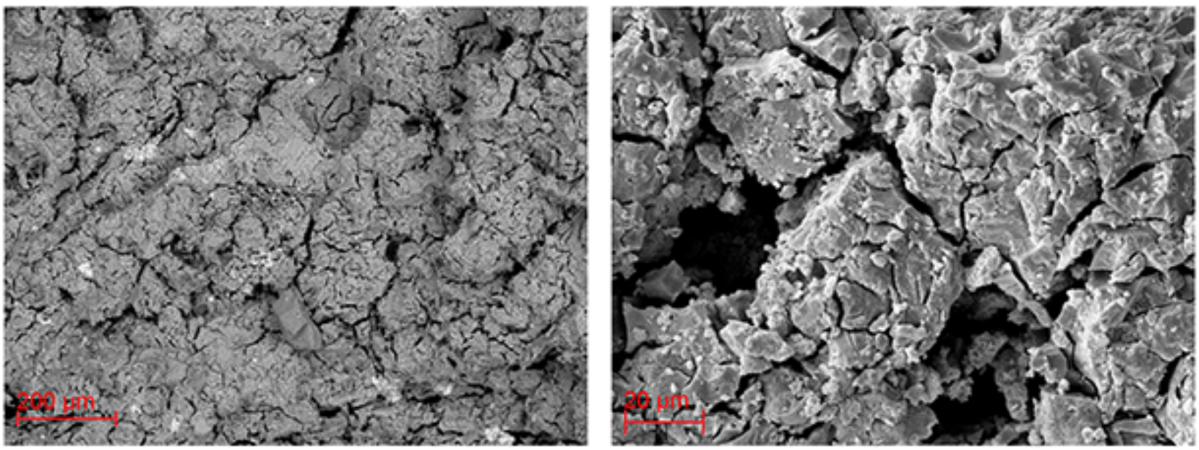

Figure 19. SEM electron images of black ash Na-silicate/NaOH sample after 90 days of hydration.

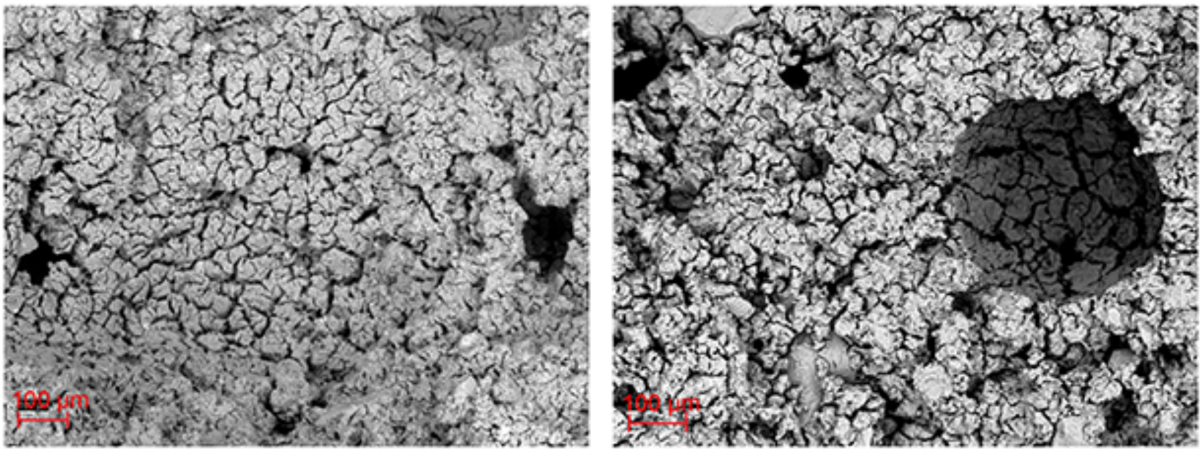

Figure 20. Comparison between SEM electron images from black ash Na-silicate sample after 90 days of hydration, shot in variable pressure and high vacuum modes, respectively.

Energy dispersive analysis of gel-masses in Na-silicate activated samples (Figure 21 and 22.) shows composition dominated by SiO_2, Na_2O, CaO, Al_2O_3, which indicates formation of Ca-Al-Na-Silicate geopolymer. However, the composition of the gel-masses varies from point to point suggesting that different original silicate and/or Al-phases phases were incorporated in polymerization.

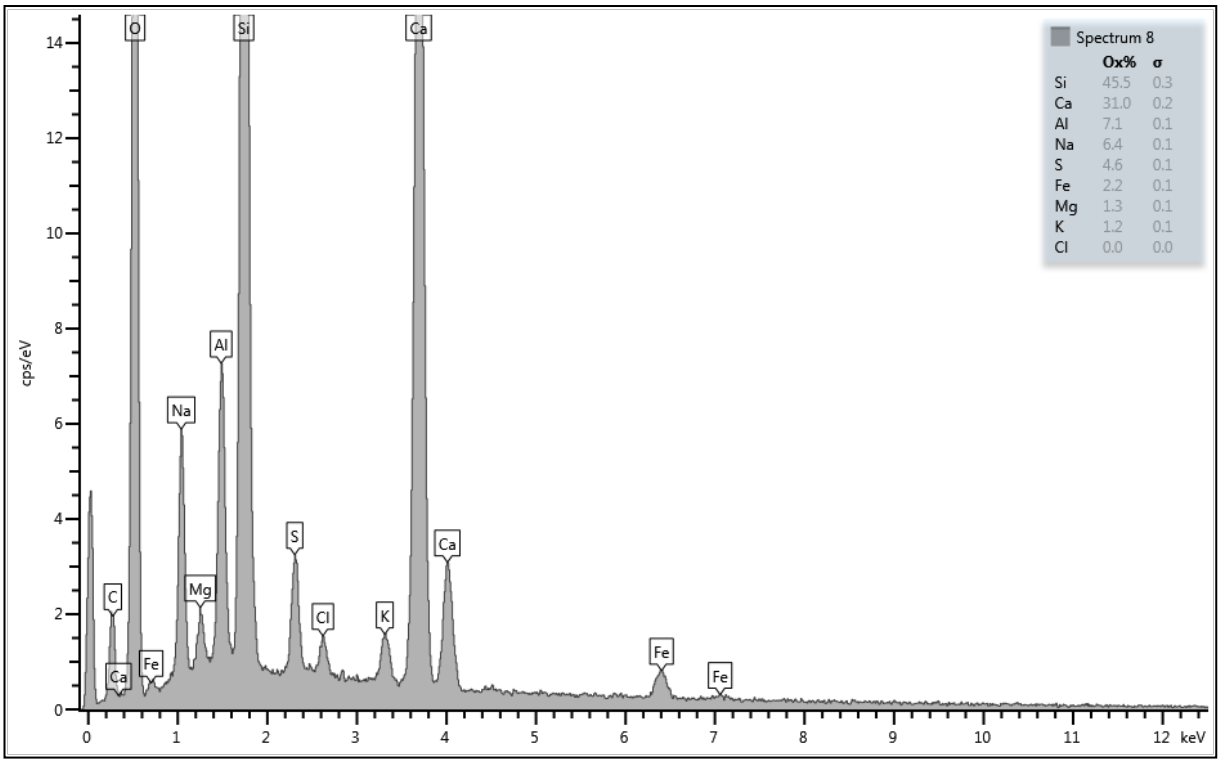

Figure 21. Energy dispersive spectrum of Ca-Na-Al-silicate gel matrix in Na-silicate treated sample after 90 days.

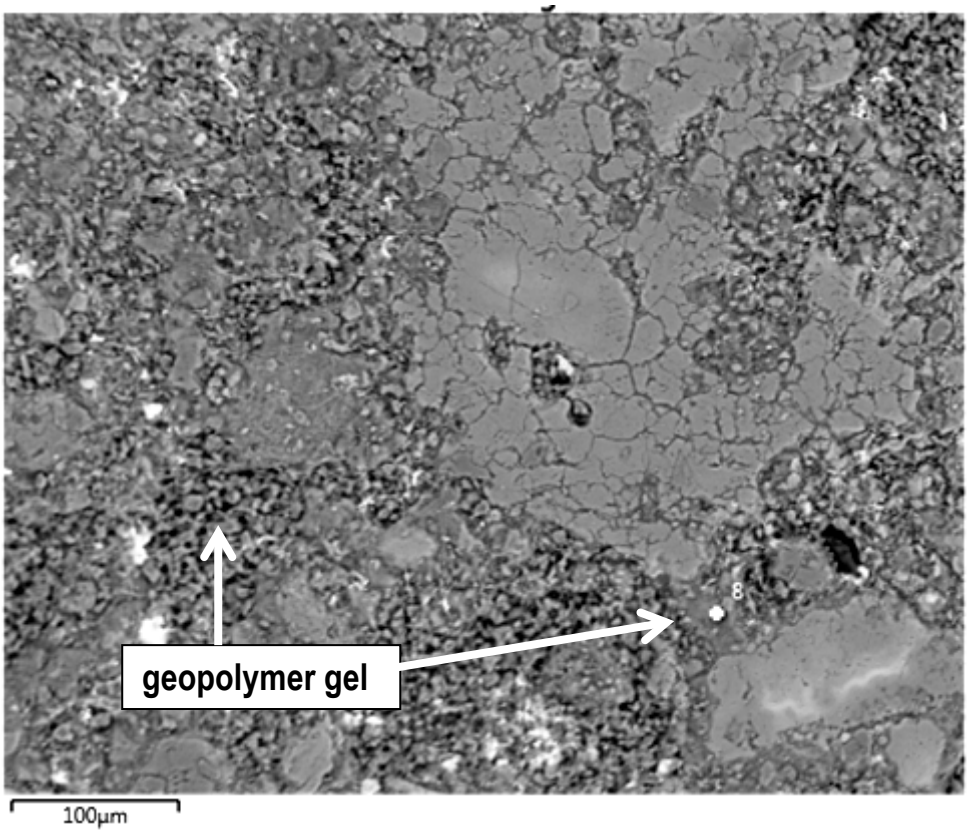

Figure 22. SEM electron (BSE) image of uncrushed, polished Na-silicate treated sample after 90 days, used for energy dispersive analysis. Grained black/grey areas are geopolymer patches.

Discussion

All mixtures exhibited remarkably different behavior in uniaxial compression strength development during the experiment (Figure 23).

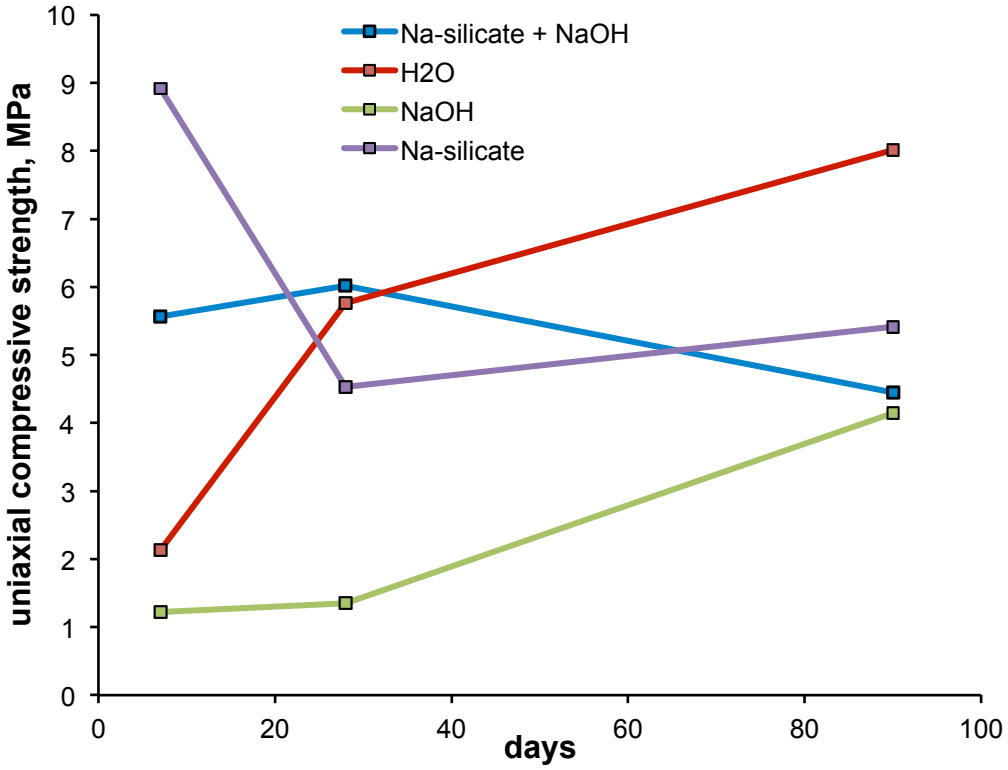

Figure 23. Development of strength in studied mixtures. The lines indicate average of three replicas measured after 7, 28 and 90 days of curing.

Original black ash contains several reactive phases that are capable of reacting with water and/or NaOH, and Na-silicate to form cementitious bonds in the material. On reactions with water, several hydration reactions occur. First of all, the Cao (lime) reacts quickly with water, forming portlandite $Ca(OH)_2$. In open conditions where atmospheric CO_2 can enter the material the portlandite reacts and forms secondary Ca-carbonate that was indicated in mineralogical changes as well as observed in scanning electron microscopy analysis. In water mixed samples secondary Ca-Al-sulphate phase (ettringite) and Ca-Al-phase (hydrocalumite) also started to precipitate. Ettringite and hydrocalumite formation is a typical to authigenic mineral precipitation processes characteristic to hydrated oil shale ash and semi-coke deposits (e.g. Mõtlep et al. 2007, Mõtlep et al. 2010, Sedman et al. 2012a,b, Sedman, 2013, Talviste, 2014). Sulphate,needed for ettringite formation was possibly delivered by CaS dissolution that disappeared quickly after the beginning of the experiments. However, earlier study of black

ash hydration (Talviste et al., 2013) did not observed massive ettringite formation (<5%). In our experiment the content of ettringite was not very high as well (max 7.6%), especially compared to normal oil shale ash and semicoke where ettringite can form up to 30% of crystalline phases (Mõtlep et al., 2007), but still noticeable. On the other hand, the SEM images of water treated samples show that nearly all pore space in the material is filled with needle-like crystals, typical to ettringite while mineralogical analysis does not support this observation. Talviste et al (2013) noted, however, that it is possible that amorphous monosulphate and/or Ca monosulphate-aluminate hydrate had precipitated together with ettringite (Baur et al. 2004). This phase is not detectable by XRD method, but is morphologically similar to ettringite. Nevertheless, it is important to note that development of ettringite, hydrocalumite and possibly amorphous monosulphate phase ensures quite good cementation of the material.

It is characteristic to black ash and water mixtures, that the material compression curves show after 7 and 28 days high residual strength ("elastic" behaviour) of the material and development of brittle properties after 90 days of curing (Figure 24).

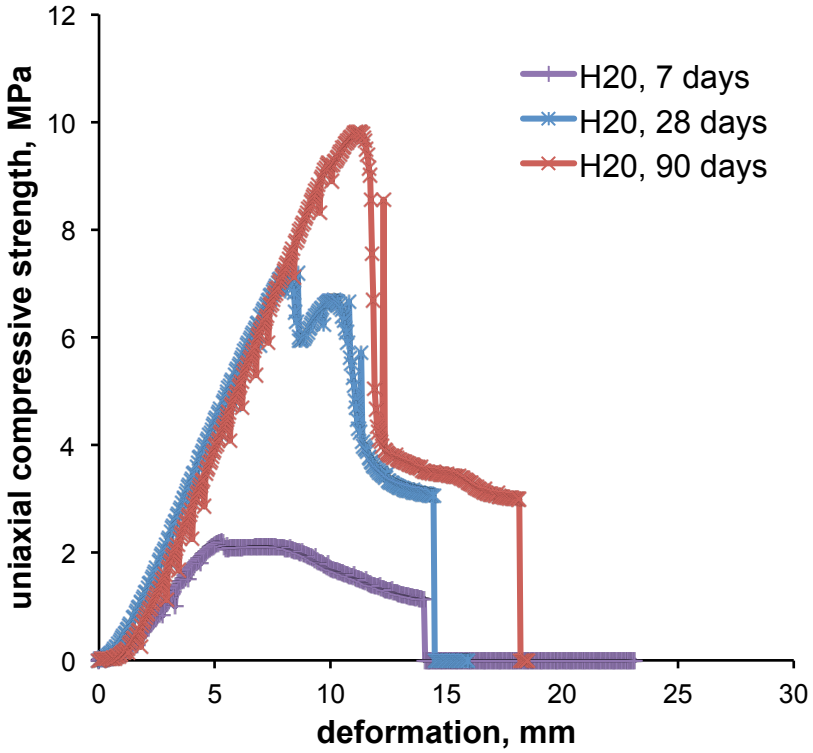

Figure 24. Compression curves of black ash – water mixtures after 7, 28 and 90 days

Mineralogical composition as well as the development of compressive strength in samples activated with NaOH dilution are rather similar to the ones mixed with water, though the final

strength is lower and it is achieved more slowly, and there is no ettringite observed in XRD nor SEM analysis of this mixture. In NaOH activated samples the material shows high residual strength and plastic/ductile deformation after 7 and 28 days, and more brittle properties are obtained after 90 days of curing (Figure 25).

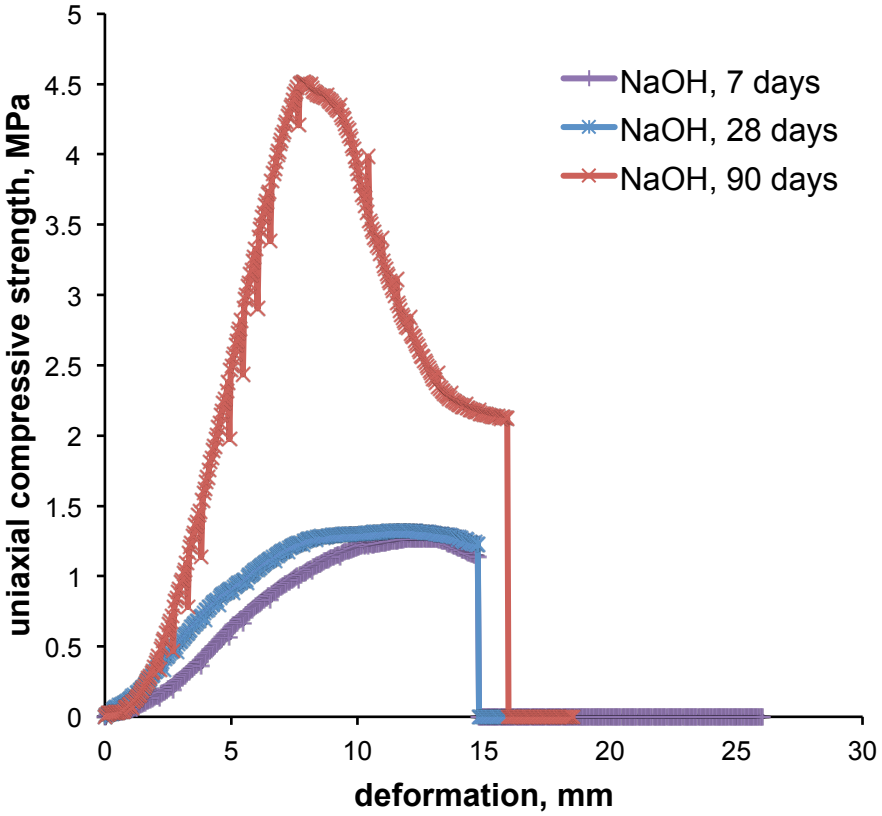

Figure 25. Compression curves of black ash – NaOH mixtures after 7, 28 and 90 days

It is possible that the lower compressive strength values of the NaOH activated samples specifically in the first stages of the experiment and in final values compared with water mixtures are due to absence of needle like ettringite or monosulphate that forms a rigid connection between ash particles. Platy crystals of hydrocalumite, however do not provide this kind of interlocking. It is possible that the increase in strength by 90 days of curing is due to the formation of amorphous geopolymer phase indicated by increase in amorphous phase, but it is not fully clear if this is the reason and geopolymerization really occurs.

Na-silicate and Na-silicate/NaOH activated samples are remarkably different form water mixture and NaOH activated samples. Both of them show high strength values already after 7 days of curing reaching up to 10.4 MPa in Na-silicate activated ash, and 7.75 MPa in Na-

silicate/NaOH, respectively. However, in the second case the values did not change much with extended curing time, and in the first case the values dropped significantly after curing for 28 days with slight improvement after 90 days (Figure 23). Both materials show characteristic brittle behaviour after 7 days of curing (Figures 26 and 27). After 28 days the materials exhibit some residual strength ("plasticity") and again slightly more brittle properties after 90 days of reaction.

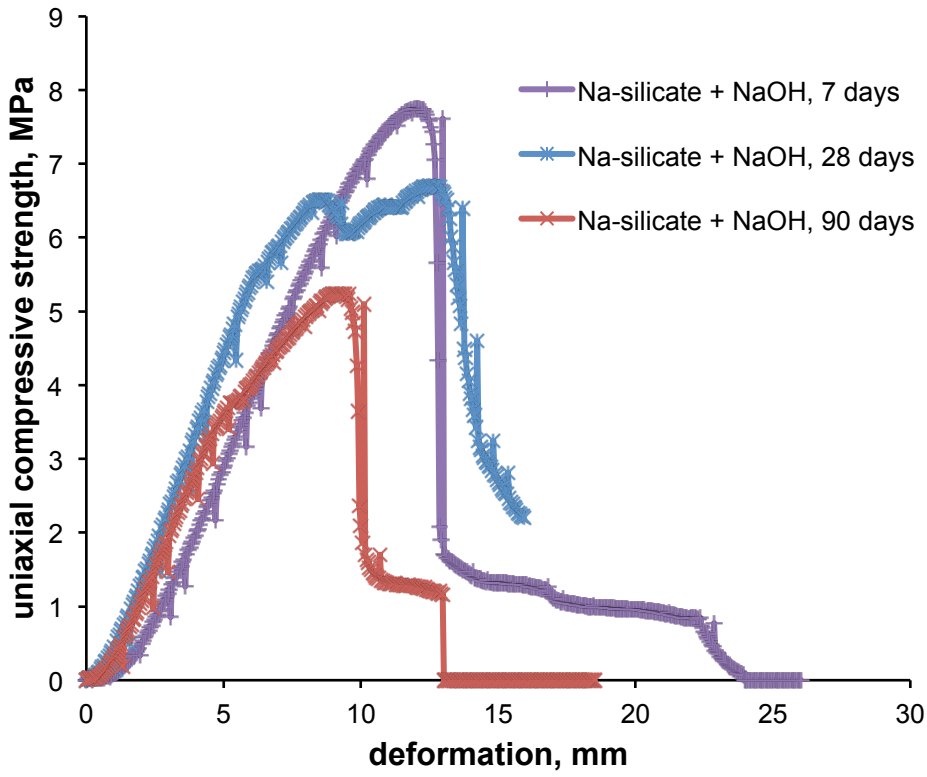

Figure 26. Compression curves of black ash – Na-silicate/NaOH mixtures after 7, 28 and 90 days of curing.

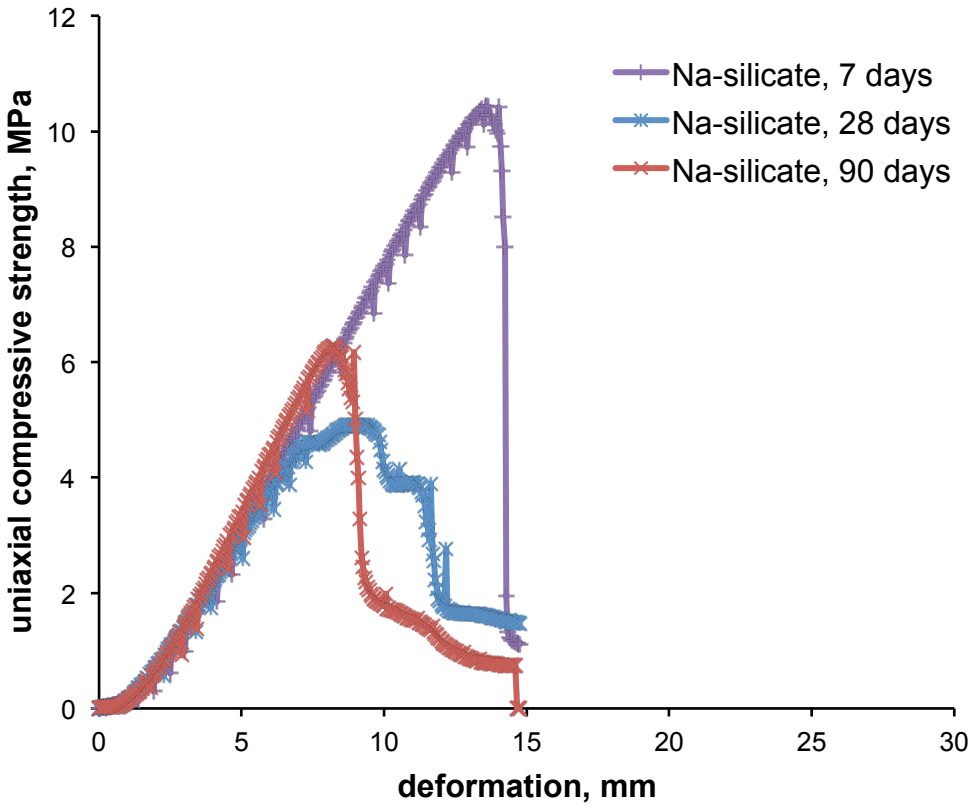

Figure 27. Compression curves of black ash – Na-silicate mixtures after 7, 28 and 90 days

The initial good compressive strength of these mixtures is provided by Ca-Na-Al-silicate gel formation in the pore space of the ash aggregate. However, already after 7 days the microstructure of these gels shows development of dense crack systems that penetrate samples, as evident from SEM images.

Considerable loss of the compressive strength or inhibition of the strength develompent in test samples made using Na-silicate and Na-silicate/NaOH as mixtrure activators after initailly relatively high strength values at 10 and 7.5 MPa after 7 days of curing is evidently related to strong dry-shrinkage of the geopolymer pastes. Shrinkage of the Na-silicate activator pastes was about 10% of the original diamteter of the test samples. Shrinkage of the test samples prepared from mixtures with Na-silicate/NaOH activator was less, but still 5% of the original dimensions after curing at ambient conditions.

Shrinkage as the decrease in volume is a very common phenomenon in ordinary concrete (Gilbert, 2002) and in geopolymers (Wallah, 2009). Gilbert (2002) distinguished several types of shrinkage: plastic shrinkage, chemical shrinkage, thermal shrinkage and drying shrinkage:

- plastic shrinkage is typical in wet concrete or when the concrete is still in plastic state due to loss of water by evaporation or infiltration into the soil/surrounding materials, which could lead to significant cracking during setting of the concrete. Plastic shrinkage depends on the cement content of the mix and the water cement ratio. It is greater for greater cement content and low water cement ratio. It is also affected by environmental conditions as temperature and humidity (Neville, 2000);

- chemical shrinkage of the concrete is caused by different chemical reactions within the cement paste, including the hydration;

- thermal shrinkage, which is related to the heat formation upon hydration of reactive phases as lime (CaO) when the material reacts with water;

- drying shrinkage is the reduction in volume which is primarily caused by the loss of water during the drying process. Drying shrinkage normally accounts for the biggest proportion of the total long-term shrinkage in concrete and geopolymers.

Factors which affect the drying of mortars also affect the magnitude and rate of development of drying shrinkage. Those factors include the type and content of cement or geopolymer binder/activator, water content and water to cement ratio, type of aggregate, maximum size and its proportion in the concrete, relative humidity and the size and shape of the member (Gilbert, 2002).

Wallah (2009) showed that in geopolymers the shrinkage is primarily affected by curing temperature and liquid-to-ash ratio. He suggested that a strong geopolymer with a smaller shrinkage can be produced at high curing temperature and the shrinkage increased significantly with the increase in liquid-to-ash ratios from 0.4 to 0.7. As the result, the increase in shrinkage is associated with the low strength development of geopolymers. More importantly, Wallah (2009) concluded that the effect of NaOH concentration on strength is small but on shrinkage is quite significant. He found that high NaOH concentration of 12.5 M produces a geopolymer with high shrinkage comparing to that with a low NaOH concentration of 7.5 M, and also the geopolymer with a high sodium silicate-to- NaOH ratio

of 3.0 gives low drying shrinkage comparing to other geopolymers with the sodium silicate-to-NaOH ratios of 0.3-1.5.

Our samples were cured at ambient conditions in lab environment and therefore the drying of Ca-Na-Al-silicate gel matrix was slow and therefore led to significant loss in volume and development of drying cracks. Though the liquid-to-ash ratio in our samples was about 0.5, which is not very high (Wallah, 2009), it still led to the shrinkage and significantly reduced strength. It is possible that curing at higher temperatures (e.g. 70 °C) would improve the performance of the ash and Na-silicate activated pastes.

Conclusions

Up to the present day amounts of the black ash residue produced at Estonian shale oil retorting plants have been relatively small. However the shale oil producers in Estonia are shifting their focus to a new and more powerful type of solid heat carrier (SHC) retorts. In the next few decades, oil production could potentially go up to a million tonnes per year as a result of new oil production retorts that are planned for production by Estonian Energy and VKG companies.

Consequently the amount of black ash type of waste increases in the future. In the current thesis a new method, geopolymerization of the black ash residue to produce possible cementitious phases, was tested. Different kind of mortars were mixed to study and evaluate the potential use of solid heat carrier ash for geopolymer type mortar and cement production and to compare alkali activated black ash with the self-cementation of the same material obtained upon hydration with plain water.

Results of the current study show that fresh black ash samples hydrated with plain water follow a steady growth trend in strength development during the curing period of 90 days, with uniaxial compressive strength values reaching up to 8 MPa after 90 days of curing. XRD mineralogical analysis and SEM imagery shows that the reason of high strength in water hydrated samples could be the formation of secondary Ca-Al-sulphate (ettringite, monosulphate) and hydrocalumite . Ettringite/monosulphate form needle like structures that fill the pore space and interlock with each other to form a strong structural matrix.

Samples activated with NaOH dilution on the other hand do not follow this kind of growth in strength. We believe that the reason for this strength behaviour could be the formation of hydrocalumite phase instead of ettringite/monosulphate phase that formed in the samples hydrated with water. Hydrocalumite forms platy crystals that do not interlock as ettringite needle like structures do. Compressive strength started to rise only after 28 days from activation and peaked clearly at 90 days. Reasons for this kind of behavior could be the formation of amorphous geopolymer phase indicated by the increase in amorphous phase after 90 days, but it is not fully clear if this is the reason.

Na-silicate and Na-silicate/NaOH activated samples showed a remarkably different strength development and mineralogical composition than samples mixed with water or NaOH. Both mixtures showed very high compressive strength values already after 7 days of curing, reaching up to 10.4 MPa in Na-silicate activated ash, and 7.75 MPa in Na-silicate/NaOH, respectively. The initial good compressive strength of these mixtures is provided by Ca-Na-Al-silicate gel forming in the pore space of the ash aggregate, that is absent in samples formed with water or NaOH. However already after 7 days the microstructure of these gels show development of dense crack systems that penetrate the samples, resulting a in remarkable drop in compressive strength. Reasons for these micro-deformations are evidently related to strong dry-shrinkage of the geopolymer pastes. Shrinkage of the Na-silicate activator pastes was about 10% of the original diameter of the test samples.

The cause of this dry shrinkage in Na-silicate activated samples is at the moment unknown. Wallah (2009) suggests that the shrinkage in geopolymers is primarily affected by curing temperature and liquid-to-ash ratio. Therefore it is possible that a geopolymeric material with smaller shrinkage and higher strength could be produced at high curing temperature (e.g. 70 °C). For the creation of usable geopolymeric binders from black ash type waste, further research is needed on the causes and prevention of Ca-Na-Al-silicate gel shrinkage.

Acknowledgements

I wish to express my gratitude to my supervisors and Annete Talpsep for guiding through this complicated theme and everyone who helped with laboratory work mixing and preparing test samples.

Põlevkiviõli tahkesoojuskandja tehnoloogia tuha geopolümeeride omadused: mineraloogia, keemia ja üheteljeline survetugevus

Tahke soojuskandja meetodil õlitootmise tahke jäätme (musta tuha) osakaal on võrreldes soojus-elektrijaamades tekkiva tuhaga siiani olnud väike, kuid viimaste aastate energeetikapoliitilised otsused ja majanduskeskkonna seisund (nafta jätkuvalt kõrge hind maailmaturul) on tõstnud huvi õlitootmise vastu. Eesti põlevkiviõli suurtootjad - Eesti Energia ja Viru Keemia Grupp ning Kiviõli Keemiatööstuse OÜ on viimastel aastatel suuremahuliselt investeerinud õlitootmistehnoloogiasse ja käivitanud või käivitamas suure tootlikkusega tahke soojuskandja tehnoloogiat kasutavaid süsteeme - nt Eesti Energia Enefit ja Viru Keemia Grupi Petrotert tehnoloogia. Seega on paratamatu selle õlitootmistehnoloogia jäätmete osakaalu kasvamine. Samuti peab arvestama, et õlitööstuse jäätmete osakaal kasvab seoses vanade keskkonnahoolimatute tolmpõletuskatelde sulgemisega 2016. aastast.

Eesti põlevkivitööstuse tuhajäätmetest taaskasutatakse alla 10%. Traditsiooniliste tuha kasutsalade kõrval on viimasel aastakümnel hakatud enam rääkima geopolümeeridest, mis on leeliskeskkonnas aktiveeritud (polümeriseeritud) madalatemperatuurilised Si-Al-klaasid.

Käesoleva uuringu eesmärgiks oli uurida võimalusi musta tuha kasutamiseks geopolümeerse mördi ja tsemendi tootmiseks. Lisaks võrreldi leelisaktiviseeritud musta tuhka ja musta tuha veega hüdratidseerimisel tekkivat tsementeerumist. Uuringu tulemused näitavad, et veega segatud musta tuha katsekehade survetugevus kasvas ühtlaselt kogu 90 päevase katseperioodi vältel. Pärast 90 päeva möödumist oli katsekehade survetugevuseks kuni 8 MPa. Mineraloogiline XRD analüüs ja SEM uuring näitavad, et tsementatsioon veega hüdratiseeritud segudes võib olla tingitud sekundaarse Ca-Al-sulfaadi mineraalide ettringiidi/monosulfaatide moodustumisest, mis loob nõeljad struktuurid, täites kogu pooriruumi ja põimudes läbi üksteise moodustades ühtlase tugeva karkassi.

NaOH abil aktiveeritud katsekehad nii kõrget survetugevust ei saavutanud. Erinevalt veega segatud proovidest, ei kasvanud NaOHga segatud katsekehade survetugevus 7 ja 28 päeva vahel ning väike survetugevuse kasv tekkis alles üheksakümnendaks päevaks. Võib oletada, et sellise tugevuse kujunemise põhjustab katsekehades ettringiidi/monosulfaadi asemel moodustunud hüdrokalumiit. Hüdrokalumiit moodustab nõeljate struktuuride asemel plaatjaid kristalle, mis ei põimu omavahel läbi ning ei moodusta tugevat karkassi nagu lihtsalt veega

segatud proovides. Survetugevuse kasvu pärast 28 päeva möödumist võib selgitada amorfse geopolümeerse faasi moodustumine, mis avaldub suurenenud amorfse faasi sisalduses, kuid see järeldus vajab edasist kontrollimist.

Na-silikaadi ja Na-silikaadi ning NaOHga aktiveeritud katsekehade tugevusomadused ja mineraalne koostis erinesid põhimõtteliselt vee või NaOHga segatud proovide omadustest. Mõlemad segud saavutasid pärast 7t päeva kõrge survetugevuse. Ainult vesiklaasiga aktiveeritud proovid kuni 10.4 MPa ja vesiklaasi ning NaOH seguga aktiveeritud proovid kuni 7.75 MPa. Katsekehade algse suure survetugevuse põhjustas Ca-Na-Al-silikaatgeeli tekkimine, mis täidab tuhast moodustunud agregaadi pooriruumi. Selline geel/klaasjas mass puudus vee või NaOHga segatud proovides. Samas, peale 7t päeva tekkisid selles geelis mikrodeformatsioonid, mis nõrgestasid märgatavalt katsekehi. Selliste mõrade põhjustajaks on suur mahukahanemine - silindrikujuliste katsekehade diameeter kahanes katse käigus kuni 10%.

Sellise mahukahanemise põhjused ei ole hetkel veel teada. Wallah (2009) pakkus välja, et geopolümeeride mahukahanemine on seotud temperatuuriga kuivamise perioodil ja segude vedeliku-tuha suhtega. Madalatel temperatuuridel on mahukahanemine soodustatud ja kuna uuritud katsekehi hoiti kivinemise perioodil toatemperatuuril, siis võis ka see olla pragunemise põhjuseks. Seega võib eeldada, et kõrgemal temperatuuril (70 °C) on võimalik toota geopolümeerset materjali, mille mahukahanemine on väiksem ning survetugevus suurem. Edasised uuringud peavad selgitama Ca-Na-Al-silikaat geeli mahukahanemise põhjused ja leidma võimalikud lahendused selle ennetamiseks.

References

Baur, I., Keller, P., Mavrocordatos, D., Wehrli, B., Johnson, C.A., 2004. Dissolution-precipitation behaviour of ettringite, monosulfate, and calcium silicate hydrate. Cement and Concrete Research, 34(2), 341–348

Craig, J.R., Vaughan, D.J., Skinner, B.J., 2001. Resources of the earth: origin, use, and environmental impact, Third edition. Prentice Hall, Upper Saddle River, New Jersey, p. 520.

Davidovits, J., 2011. Geopolymer Chemistry and Applications, 3rd Edition. Institut Géopolymére, France.

Duxson, P., Fernandez-Jimenez, A., Provis, J.L., Lukey, G.C., Palomo, A., van Deventer, J.S.J. 2006. Geopolymer technology: the current state of the art. Journal of Materials Science, 42(9), 2917 - 2933.

Eesti Energia Õlitööstus AS, 2013. Õlitehase maa-ala detailplaneeringu keskkonnamõju strateegilise hindamise aruanne. http://www.energiatalgud.ee/img_auth.php/0/01/P%C3%B6yry._%C3%95litehase_maa-ala_detailplaneeringu_KSH_aruanne_.pdf

Gilbert, R. I., 2002. Creep and shrinkage models for high strength concrete - proposal for inclusion in AS3600. Australian Journal of Structural Engineering, 4(2), 95-106.

Golubev, N., 2003. Solid heat carrier technology for oil shale retorting. Oil Shale, 20 (3S), 324-332.

Hanni, R., 1996. Energy and valuable material by-product from firing Estonian oil shale. Waste Management, 16, 97–99.

Kaasik, A., Vohla, C., Mõtlep, R., Mander, Ü., Kirsimäe, K., 2008. Hydrated calcareous oil-shale ash as potential filter media for phosphorus removal in constructed wetlands. Water Research, 42, 1315–1323.

Kattai, V., Saadre, T., Savitski, L., 2000. Estonian oil shale. Geological Survey of Estonia,

Koel, M., 1999. Estonian oil shale. Oil Shale Extra: http://www.kirj.ee/public /oilshale/Est-OS.htm, last accessed April 8, 2013.

Kõiv, M., Liira, M., Mander, Ü., Mõtlep, R., Vohla, C., Kirsimäe, K., 2010. Phosphorus removal using Ca-rich hydrated oil shale ash as filter material - The effect of different phosphorus loadings and wastewater compositions. Water Research, 44, 5232–5239.

Mindess, S., Young, J.F., Darwin, D., 2003. Concrete (2nd Edition), Prentice-Hall, Upper Saddle River, New Jersey, USA

Mõtlep, R., Kirsimäe, K., Talviste, P., Puura, E., Jürgenson, J., 2007. Mineral composition of Estonian oil shale semi-coke sediments. Oil Shale, 24, 405–422.

Mõtlep, R., Sild, T., Puura, E., Kirsimäe, K., 2010. Composition, diagenetic transformation and alkalinity potential of oil shale ash sediments. Journal of Hazardous Materials, 180, 567–573.

Neville, A. M., 2000. Properties of Concrete (Fourth and Final ed.). Essex, England: Pearson Education, Longman Group

Ots, A., 2006. Oil Shale Fuel Combustion. Tallinna Raamatutrükikoda, Tallinn, p.833.
Paat, A., 2002. About the mineral composition of Estonian oil shale ash. Oil Shale, 19, 321–333.

Pets, L., Knot, P., Haldna, J., Shvenke, G., Juga, R., 1985. Trace elements in kukersite oil shale ash of Baltic Power Plant. Oil Shale, 2, 379–390.

Sedman, A., 2013. Strength and self-cementing properties of oil shale retorting wastes. PhD Thesis in Geology. University of Tartu.

Sedman, A., Talviste, P., Kirsimäe, K., 2012b. Hydration and carbonation reactions and corresponding changes in permeability properties of co-deposited oil shale ash and semi-coke waste materials in a small-scale field experiment. Oil Shale, 29, 279– 294.

Sedman, A., Talviste, P., Mõtlep, R., Jõeleht, A., Kirsimäe, K., 2012a. Geotechnical characterization of Estonian oil shale semi-coke deposits with prime emphasis on their shear strength. Engineering Geology, 131, 37–44.

Soone, J., Doilov, S., 2003. Sustainable utilization of oil shale resources and comparison of contemporary technologies used for oil shale processing. Oil Shale, 20 (3S), 311-323.

Statistics Estonia, 2010. Statistical Yearbook of Estonia. Tallinn: Statistics Estonia.
Tallinn, p. 226. (in Estonian).

Talviste, P., 2014. Temporal changes in weak natural and artificial soils – influence on geotechnical characteristics. PhD Thesis in Geology. University of Tartu.

Talviste, P., Sedman, A., Mõtlep, R., Kirsimäe, K., 2013. Self-cementing properties of oil shale solid heat carrier retorting residue. Waste Management & Research, 31, 1-7

Teedumäe, A., Raukas, A., 2006. The possibility of integrating sustainability into legal framework for use of oil shale reserves. Oil Shale, 23(2), 119 - 124.

Wallah, S., 2009. Drying Shrinkage of Heat-Cured Fly Ash-Based Geopolymer Concrete. Modern Applied Science.

World Energy Council 2010. Oil shale. In: Clarke AW and Trinnaman JA (eds) 2010 Survey of Energy Resources. London: World Energy Council, pp. 93–123.

Supplements

Table 3. Mineral composition, t%; tr – trace amount |<0.5%

	Black ash	Black ash + water			black ash + NaOH			Black ash + Na-silicate/NaOH			Black ash + Na-silicate		
phase/days	original	7	28	90	7	28	90	7	28	90	7	28	90
Quartz	11.7	11.7	11.9	10.7	10.1	13.3	8.4	8.7	10.6	7.7	7.4	6.7	7.8
Orthoclase	14.3	12.5	11.3	12.3	12.0	11.5	10.0	11.2	10.9	10.5	11.8	10.4	12.1
Muscovite/mica	2.6	1.7	3.4	5.7		1.5	5.1	5.9	6.6	7.1	6.9	7.1	7.2
Calcite	26.8	23.2	28.4	25.6	23.6	25.8	21.7	19.6	21.6	21.0	18.9	16.5	19.2
Vaterite		2.9	tr	1.5	2.4	2.7	2.9	1.4	1.3	1.5	1.5	1.9	2.1
Dolomite	8.5	8.6	11.8	6.0	6.6	7.1	4.7	5.7	3.9	5.9	5.7	5.5	5.0
Lime	2.1												
Portlandite		1.2	tr	tr	1.5	2.1	0.7						
Periclase	7.5	2.2	1.9	1.9	2.5	2.7	2.1	3.8	3.3	2.5	3.2	2.1	2.1
C2S	3.2	5.7	6.7	7.1	5.8	6.9	6.8	2.7	2.2	2.3	2.3	2.4	2.5
Merwinite	5.2	2.2	1.6	1.3	2.8	2.8	2.4	2.6	2.9	2.1	2.0	2.3	1.5
Melilite	4.2	2.0	2.6	2.9	3.8	3.0	2.1	2.8	2.3	3.0	2.6	3.3	2.6
Wollastonite	1.5	2.5	3.1	4.3	3.8	3.4	3.1	4.0	4.7	4.9	3.7	4.3	4.2
Oldhamite	3.6				0.7	0.6	tr	2.0	1.0	0.7	1.7	0.8	0.8
Anhydrite	1.1												
Gypsum		0.9	0.7	1.0	1.0	1.3	2.3						
Hydrocalumite		13.9	6.0	11.1	17.9	13.3	16.5						
Ettringite		4.7	7.6	6.3									
Smectite					0.5	0.8	2.1						
Hematite	1.1	0.5	tr	0.6	tr	tr	tr	0.8	0.8	0.6	0.7	tr	0.8
Magnetite	0.9	1.3	1.8	1.2	1.1	1.6	1.2	0.9	1.0	0.9	0.7	0.9	0.6
Amorphous phase	5.7	2.2	tr	tr	3.7	tr	7.1	28.2	27.0	29.1	31.0	35.4	31.5

Non-exclusive licence to reproduce thesis and make thesis public

I, Peeter Paaver

1. herewith grant the University of Tartu a free permit (non-exclusive licence) to:

1.1. reproduce, for the purpose of preservation and making available to the public, including for addition to the DSpace digital archives until expiry of the term of validity of the copyright, and

1.2. make available to the public via the web environment of the University of Tartu, including via the DSpace digital archives until expiry of the term of validity of the copyright,

Geopolymerization of the Estonian oil shale solid heat carrier retorting waste ash: changes in mineral-chemical composition and uniaxial compressive strength development,

supervised by Kalle Kirsimäe and Päärn Paiste

2. I am aware of the fact that the author retains these rights.

3. I certify that granting the non-exclusive licence does not infringe the intellectual property rights or rights arising from the Personal Data Protection Act.

Tartu, **23.05.2014**